Journal of Statistical Physics, Vol. 115, Nos. 1/2, April 2004 (© 2004)

Finite-Size Scaling in the Driven Lattice Gas

Sergio Caracciolo,[1] Andrea Gambassi,[2] Massimiliano Gubinelli,[3] and Andrea Pelissetto[4]

Received April 16, 2003; accepted July 14, 2003

We present a Monte Carlo study of the high-temperature phase of the two-dimensional driven lattice gas at infinite driving field. We define a finite-volume correlation length, verify that this definition has a good infinite-volume limit independent of the lattice geometry, and study its finite-size-scaling behavior. The results for the correlation length are in good agreement with the predictions based on the field theory proposed by Janssen, Schmittmann, Leung, and Cardy. The theoretical predictions for the susceptibility and the magnetization are also well verified. We show that the transverse Binder parameter vanishes at the critical point in all dimensions $d \geqslant 2$ and discuss how such result should be expected in the theory of Janssen *et al.* in spite of the existence of a dangerously irrelevant operator. Our results confirm the Gaussian nature of the transverse excitations.

KEY WORDS: Driven lattice gas; finite-size scaling; critical behavior; nonequilibrium statistical mechanics.

1. INTRODUCTION

At present, the statistical mechanics of systems in thermal equilibrium is quite well established. On the other hand, little is known in general for nonequilibrium systems, although some interesting results have been recently obtained.[1] It seems therefore worthwhile to study simple models

[1] Dipartimento di Fisica and INFN, Università di Milano, and INFM-NEST, I-20133 Milano, Italy; e-mail: sergio.caracciolo@mi.infn.it

[2] Max-Planck-Institut für Metallforschung, Heisenbergstr. 3, D-70569 Stuttgart, Germany, and Institut für Theoretische und Angewandte Physik, Universität Stuttgart, Pfaffenwaldring 57, D-70569 Stuttgart, Germany; e-mail: gambassi@mf.mpg.de

[3] Dipartimento di Matematica Applicata and INFN, Università di Pisa, I-56100 Pisa, Italy; e-mail: m.gubinelli@dma.unipi.it

[4] Dipartimento di Fisica and INFN, Università di Roma "La Sapienza," I-00185 Roma, Italy; e-mail: Andrea.Pelissetto@roma1.infn.it

0022-4715/04/0400-0281/0

which are out of thermal equilibrium. One of them was introduced at the beginning of the eighties by Katz *et al.*,[2] who studied the stationary state of a lattice gas under the action of an external drive. The model, hereafter called driven lattice gas (DLG), is a kinetic Ising model on a periodic domain with Kawasaki dynamics and biased jump rates. Although not in thermal equilibrium, the DLG has a stationary state and shows a finite-temperature phase transition, which is however different in nature from its equilibrium counterpart.[5]

Despite its simplicity, the DLG has not yet been solved exactly[6] and at present there is still much debate on the nature of the phase transition.[6–12] In refs. 6 and 7, Janssen, Schmittmann, Leung, and Cardy (JSLC) developed a continuum theory which should capture the basic features of the transition and which provides exact predictions for the critical exponents. Several computer simulations in two and three dimensions[13–16] provided good support to these field-theoretical predictions, once it was understood that the highly anisotropic character of the transition required some kind of anisotropic finite-size scaling (FSS).[14, 17] Still some discrepancies remained, prompting Garrido, de los Santos, and Muñoz[8–10] to reanalyze the derivation of the field theory. On the basis of this analysis, they suggested that the DLG at infinite driving field should not behave as predicted by JSLC but should rather belong to the universality class of the randomly driven lattice gas (RDLG).[18, 19] This approach gives different predictions for the critical exponents that have been apparently verified numerically,[20, 21] see also ref. 22.

In view of these contradictory results, a new numerical investigation is necessary, in order to decide which theory describes the critical behavior of the DLG. For this purpose it is useful to consider quantities that are exactly predicted at least in one of the two theories. Here we shall focus on transverse fluctuations since in the JSLC theory transverse correlation functions are predicted to be Gaussian. Therefore, beside critical exponents, one can also exactly compute the FSS functions of several observables and make an unambiguous test of the JSLC theory.

A basic ingredient of our FSS analysis is the finite-volume correlation length. In spite of the extensive numerical work, no direct studies of the correlation length have been done so far, essentially because it is not easy to define it. Indeed, in the high-temperature phase the model shows long-range correlations due to the violation of detailed balance.[23, 24] Therefore,

[5] For an extensive presentation of the DLG and of many generalizations, see refs. 3 and 4.

[6] The DLG is soluble for infinite drive in the limit in which jumps in the direction of the field are infinitely more frequent than jumps in the orthogonal directions.[5]

no correlation length can be defined from the large-distance behavior of the two-point correlation function. A different definition is therefore necessary: In ref. 25 a parallel correlation length is defined. However, this definition suffers from many ambiguities (see the discussion in ref. 3) and gives results for the exponent $\nu_{\parallel}$ which are not in agreement with the JSLC theory.[13] Even more difficult appears the definition of a transverse correlation length because of the presence of negative correlations at large distances.[3, 13]

In this paper we define a finite-volume transverse correlation length generalizing the definition of the second-moment correlation length that is used in equilibrium systems. Because of the conserved dynamics, such a generalization requires some care. Here, we use the results of ref. 26. The main advantage of using a correlation length is the possibility of performing FSS checks without free parameters. We find that the susceptibility and the correlation length show a FSS behavior that is in full agreement with the idea that transverse fluctuations are Gaussian. This immediately implies the JSLC predictions $\gamma_{\perp} = 1$ and $\nu_{\perp} = 1/2$. We also study the FSS behavior of the magnetization, finding $\beta_{\perp}/\nu_{\perp} = 1.023(43)$, in agreement with mean-field behavior. Finally, we consider the transverse Binder parameter and find that it goes to zero at T_c (the critical temperature) as the volume increases. This supports again the Gaussian nature of the transverse mode and, as we discuss in detail, it is not in contradiction with the presence of a dangerously irrelevant operator. Indeed, since no zero mode is present in the theory, there should be no anomalous scaling.

The paper is organized as follows. In Section 2 we describe the model and define the observables measured in the Monte Carlo simulation. Section 3 reviews the FSS theory and introduces the basic formulae that are used in the analysis of the numerical data. Next in Section 4, we consider the field theory of refs. 6 and 7 in a finite geometry and compute the FSS functions for several observables. In Section 5 we describe the simulations and present the results which are then discussed and compared with recent findings[20, 21] in Section 6. We confirm the field-theoretical predictions of JSLC both for infinite-volume quantities and for the finite-size behavior. In Appendix A we consider the $O(N)$ model for $N \to \infty$ above the upper critical dimension and discuss the critical behavior of different definitions of the Binder parameter. In particular, we show that, if it is defined in terms of correlation functions at nonzero momenta, then it vanishes for all $d \geqslant 4$: this is the same behavior as that expected in the DLG for $d \geqslant 2$ on the basis of the JSLC theory and verified numerically for $d = 2$. In Appendix B we sketch a one-loop calculation of the Binder parameter in the JSLC theory. A short account of the results presented in this work has been given in ref. 27.

2. DEFINITIONS

2.1. The Model

We consider a finite square lattice Λ and N particles, each of them occupying a different lattice site. A configuration of the system is specified by the set of occupation numbers of each site $n = \{n_i \in \{0, 1\}\}_{i \in \Lambda}$. The standard lattice gas is characterized by a nearest-neighbor attractive ("ferromagnetic" in spin language) Hamiltonian

$$H_\Lambda[n] = -4 \sum_{\langle i, j \rangle \in \Lambda} n_i n_j, \tag{1}$$

where the sum runs over all lattice nearest neighbors. We consider a discrete-time Kawasaki dynamics,[28] which preserves the total number of particles N or, equivalently, the density

$$\rho_\Lambda \equiv \frac{1}{|\Lambda|} \sum_{i \in \Lambda} n_i, \tag{2}$$

where $|\Lambda|$ is the total number of sites in Λ. At each step, we randomly choose a lattice link $\langle i, j \rangle$. If $n_i = n_j$, nothing happens. Otherwise, we propose a particle jump with probability $w(\Delta H/T)$, where

$$\Delta H = H_\Lambda[n'] - H_\Lambda[n] \tag{3}$$

is the difference in energy between the new (n') and the old (n) configuration. If the probability $w(x)$ satisfies

$$w(-x) = e^x w(x), \tag{4}$$

then the dynamics is reversible, i.e., satisfies detailed balance. Under these conditions there is a unique equilibrium measure given by

$$P_{\Lambda, \mathrm{eq}}[n] = \frac{e^{-\beta H_\Lambda[n]}}{\sum_{\{n'\}} e^{-\beta H_\Lambda[n']}}, \tag{5}$$

where $\beta \equiv 1/T$. In the thermodynamic limit the lattice gas exhibits a second-order phase transition for $\rho_\Lambda = 1/2$ and $\beta_c = \frac{1}{2} \ln(\sqrt{2} + 1)$, which belongs to the standard Ising universality class.

The DLG is a generalization of the lattice gas in which one introduces a uniform (in space and time) force field pointing along one of the axes of the lattice, i.e., $\mathbf{E} = E \hat{\mathbf{x}}$: It favors (respectively suppresses) the jumps of the particles in the positive (resp. negative) $\hat{\mathbf{x}}$-direction. If Λ is bounded by *rigid*

walls, then **E** is a conservative field and it can be accounted for by adding a potential term to $H_\Lambda[n]$. Therefore, the system remains in thermal equilibrium. The net effect of **E** is simply to induce a concentration gradient in the equilibrium state.

Here, we consider instead periodic boundary conditions.[7] In this case, the field **E** does not have a global potential and the system reaches a stationary state which, however, is not a state in thermal equilibrium.

In the DLG transition probabilities take into account the work done by the field during the particle jump from one site to one of its nearest neighbors. In this case one proposes a particle jump with probability $w(\beta \Delta H + \beta E \ell)$, with $\ell = (-1, 0, 1)$ for jumps (along, transverse, opposite) to $\hat{\mathbf{x}}$.

For $E \neq 0$ and $\rho_\Lambda = 1/2$, the system undergoes a continuous phase transition[3,4] at an inverse temperature $\beta_c(E)$ which saturates, for $E \to \infty$, at $\beta_c(\infty) \approx 0.71 \beta_c(0)$. For $\beta < \beta_c(E)$ particles are homogeneously distributed in space, while for $\beta > \beta_c(E)$ phase separation occurs: Two regions are formed, one almost full and the other one almost empty, with interfaces parallel to **E**.

2.2. Observables

We consider a finite square lattice of size $L_\parallel \times L_\perp$ with periodic boundary conditions (parallel and orthogonal refer to the direction of the electric field). We define a "spin" variable $s_\mathbf{j} \equiv 2n_\mathbf{j} - 1$ and its Fourier transform

$$\phi(\mathbf{k}) \equiv \sum_{\mathbf{j} \in \Lambda} e^{i\mathbf{k}\cdot\mathbf{j}} s_\mathbf{j}, \tag{6}$$

where the allowed momenta are

$$\mathbf{k}_{n,m} \equiv \left(\frac{2\pi n}{L_\parallel}, \frac{2\pi m}{L_\perp} \right), \tag{7}$$

with $(n, m) \in \mathbb{Z}_{L_\parallel} \times \mathbb{Z}_{L_\perp}$.

We consider the model at half filling, i.e., for $\rho_\Lambda = 1/2$. Then

$$\sum_{\mathbf{j} \in \Lambda} s_\mathbf{j} = 0, \qquad \text{i.e.,} \quad \phi(\mathbf{k}_{0,0}) = 0. \tag{8}$$

[7] In principle, it is enough to consider periodic boundary conditions in the field direction. The boundary conditions in the transverse directions are largely irrelevant for the problems discussed here.

In the ordered phase $|\phi(\mathbf{k})|$ takes its maximum for $\mathbf{k} = \mathbf{k}_{0,1}$, and the expectation value on the steady state of its module

$$m(\beta; L_{\parallel}, L_{\perp}) \equiv \frac{1}{|\Lambda|} \langle |\phi(\mathbf{k}_{0,1})| \rangle \tag{9}$$

is a good order parameter.

In momentum space the static structure factor, the Fourier transform of the two-point correlation function,

$$\tilde{G}(\mathbf{k}; L_{\parallel}, L_{\perp}) \equiv \frac{1}{|\Lambda|} \langle |\phi(\mathbf{k})|^2 \rangle \tag{10}$$

vanishes at $\mathbf{k}_{0,0}$ because of Eq. (8) and attains its maximum at $\mathbf{k}_{0,1}$, so that it is natural to define the susceptibility as[8]

$$\chi_{\perp}(\beta; L_{\parallel}, L_{\perp}) \equiv \tilde{G}(\mathbf{k}_{0,1}; L_{\parallel}, L_{\perp}). \tag{11}$$

We also define the four-point connected correlation function

$$\tilde{G}^{(4)}(\mathbf{k}_1, \mathbf{k}_2, \mathbf{k}_3, \mathbf{k}_4; L_{\parallel}, L_{\perp}) = \frac{1}{|\Lambda|} \langle \phi(\mathbf{k}_1)\, \phi(\mathbf{k}_2)\, \phi(\mathbf{k}_3)\, \phi(\mathbf{k}_4) \rangle_{\text{conn}}, \tag{12}$$

and the related transverse Binder cumulant $g(\beta; L_{\parallel}, L_{\perp})$ defined as

$$g(\beta; L_{\parallel}, L_{\perp}) \equiv 2 - \frac{\langle |\phi(\mathbf{k}_{0,1})|^4 \rangle}{\langle |\phi(\mathbf{k}_{0,1})|^2 \rangle^2} = -\frac{\tilde{G}^{(4)}(\mathbf{k}_{0,1}, \mathbf{k}_{0,1}, -\mathbf{k}_{0,1}, -\mathbf{k}_{0,1}; L_{\parallel}, L_{\perp})}{|\Lambda|\, [\tilde{G}(\mathbf{k}_{0,1}; L_{\parallel}, L_{\perp})]^2}. \tag{13}$$

Next, we would like to define a correlation length. In infinite-volume equilibrium systems there are essentially two different ways of doing it. One can define the correlation length in terms of the large-distance behavior of the two-point correlation function or by using its small-momentum behavior (second-moment correlation length). In the DLG the first method does not work. Indeed, in the high-temperature phase the two-point correlation function always decays *algebraically* with the distance. Moreover, it is not positive definite because of negative correlations in the transverse directions.[3] This peculiar behavior is due to the fact that in the infinite-volume

[8] We note that the susceptibility defined by using the linear response theory does not coincide in nonequilibrium systems with that defined in terms of the Fourier transform of the two-point correlation function.

limit (at fixed temperature) the static structure factor $\tilde{G}(\mathbf{k}; \infty, \infty)$ has a finite discontinuity at $\mathbf{k} = 0$.

In this paper we propose a new definition that generalizes the second-moment correlation length used in equilibrium spin systems. The basic observation is that in the DLG the infinite-volume *wall-wall* correlation function decays exponentially, i.e.,

$$\sum_{x_\parallel} G((x_\parallel, x_\perp); \infty, \infty) \equiv \int d^{d-1}q_\perp \, \tilde{G}((0, q_\perp); \infty, \infty) \, e^{iq_\perp \cdot x_\perp} \sim e^{-\kappa |x_\perp|}, \qquad (14)$$

as in equilibrium systems. This holds at tree level both in the JSLC and in RDLG field theories and to all orders of perturbation theory in the JSLC theory, see Section 4. Therefore, we can define a correlation length as in equilibrium systems, paying due attention to the conserved dynamics. Here, we follow ref. 26, where we discussed the possible definitions of correlation length in the absence of the zero mode, as it is the case here.

We consider the structure factor in finite volume at zero longitudinal momenta

$$\tilde{G}_\perp(q; L_\parallel, L_\perp) \equiv \tilde{G}((0, q); L_\parallel, L_\perp), \qquad (15)$$

(note that the conservation law implies $\tilde{G}_\perp(0; L_\parallel, L_\perp) = 0$) and define a finite-volume (transverse) correlation length[9]

$$\xi_{ij}(L_\parallel, L_\perp) \equiv \sqrt{\frac{1}{\hat{q}_j^2 - \hat{q}_i^2} \left(\frac{\tilde{G}_\perp(q_i; L_\parallel, L_\perp)}{\tilde{G}_\perp(q_j; L_\parallel, L_\perp)} - 1 \right)}, \qquad (16)$$

where $\hat{q}_n = 2 \sin(\pi n / L_\perp)$ is the lattice momentum. Since $\tilde{G}_\perp(0; L_\parallel, L_\perp) = 0$, q_i and q_j must not vanish. Moreover, as discussed in ref. 26, the definition should be valid for all β in finite volume. Since the system orders in an even number of stripes, for i even $\tilde{G}_\perp(q_i; L_\parallel, L_\perp)$ is zero as $\beta \to \infty$. Therefore, if our definition should capture the nature of the phase transition, we must require i and j to be odd. Although any choice of i, j is conceptually good, finite-size corrections increase with i, j, a phenomenon which should be expected since the critical modes correspond to $q \to 0$. Thus, we choose $(i, j) = (1, 3)$, defining $\xi_\perp \equiv \xi_{13}$.

[9] In ref. 26 we showed that any good finite-volume correlation length must satisfy two properties: (i) it must be finite for all $T \neq 0$ and $L_\perp, L_\parallel < \infty$; (ii) it must diverge as $T \to 0$ even in finite volume. The definition (16) satisfies these two properties. Note that in infinite volume one can also define a correlation length from the large-distance behavior of the correlation function, i.e., one can define $\xi_{\infty,\perp} = 1/\kappa$, where κ is defined in Eq. (14). Such a definition is not convenient here, since it does not admit a finite-volume generalization.

The same method can be used to define a longitudinal correlation length, although in this case we do not have an all-order proof (not even in the JSLC theory) that wall-wall longitudinal correlations decay exponentially. It is enough to consider the longitudinal structure factor at zero transverse momentum

$$\tilde{G}_{\parallel}(q; L_{\parallel}, L_{\perp}) = \tilde{G}((q, 0); L_{\parallel}, L_{\perp}), \tag{17}$$

and use again Eq. (16). In this case, there is no reason to avoid the use of even i or j and thus we define $\xi_{\parallel} \equiv \xi_{12}$.

Near a phase-transition point the quantities we have defined above show power-law divergences. As usual, see, e.g., ref. 3, we define transverse exponents by assuming

$$\begin{aligned} \xi_{\perp} &\sim t^{-\nu_{\perp}} \\ \chi_{\perp} &\sim t^{-\gamma_{\perp}}, \end{aligned} \tag{18}$$

for $t \equiv (\beta_c - \beta)/\beta_c \to 0^+$. The magnetization vanishes in the low-temperature phase as

$$m \sim (-t)^{\beta_{\perp}}. \tag{19}$$

3. FINITE-SIZE SCALING

In the neighborhood of a critical point the behavior of long-range observables is controlled by few quantities, corresponding in the renormalization-group language to coordinates parametrizing the relevant directions in the infinite-dimensional coupling space. When the system is finite, its size plays the role of another relevant operator. This means that an observable $\mathcal{O}$, which diverges in the thermodynamic limit as

$$\mathcal{O}_{\infty}(\beta) \sim t^{-\gamma_{\mathcal{O}}} \qquad \text{for} \quad t \equiv 1 - \frac{\beta}{\beta_c} \to 0^+, \tag{20}$$

behaves in a finite system of size $L_{\parallel} \times L_{\perp}^{d-1}$ as[29, 30]

$$\begin{aligned} \mathcal{O}(\beta; L_{\parallel}, L_{\perp}) &\approx t^{-\gamma_{\mathcal{O}}} f_{1,\mathcal{O}}(t^{-\nu}/L_{\perp}; S) \\ &\approx L_{\perp}^{\gamma_{\mathcal{O}}/\nu} f_{2,\mathcal{O}}(t^{-\nu}/L_{\perp}; S) \\ &\approx L_{\perp}^{\gamma_{\mathcal{O}}/\nu} f_{3,\mathcal{O}}(\xi_{\infty}(\beta)/L_{\perp}; S), \end{aligned} \tag{21}$$

where $\xi_{\infty}(\beta)$ is the infinite-volume correlation length and $S \equiv L_{\parallel}/L_{\perp}$ is the aspect ratio that is kept fixed in the FSS limit. From Eq. (21) we can derive

a general relation for the ratio of $\mathcal{O}(\beta; L_\parallel, L_\perp)$ at two different sizes $(L_\parallel, L_\perp)$ and $(\alpha L_\parallel, \alpha L_\perp)$. In the FSS limit we obtain

$$\frac{\mathcal{O}(\beta; \alpha L_\parallel, \alpha L_\perp)}{\mathcal{O}(\beta; L_\parallel, L_\perp)} = F_{\mathcal{O}}\left(\alpha, \frac{\xi(\beta; L_\parallel, L_\perp)}{L_\perp}, S\right), \tag{22}$$

where we have replaced $\xi_\infty(\beta)/L_\perp$ with $\xi(\beta; L_\parallel, L_\perp)/L_\perp$ by inverting $\xi(\beta; L_\parallel, L_\perp) \approx L_\perp f_{3,\xi}(\xi_\infty(\beta)/L_\perp; S)$. The function $F_{\mathcal{O}}(\alpha, z, S)$ is universal and is directly accessible numerically, e.g., by Monte Carlo simulations —no need to fix any parameter—since all quantities appearing in Eq. (22) are directly measurable. Moreover, as we shall show below, all critical exponents can be determined from the FSS functions $F_{\mathcal{O}}(\alpha, z, S)$ independently of the critical temperature.

If we define $z \equiv \xi(\beta; L_\parallel, L_\perp)/L_\perp$, then z varies between 0 and $z^*(S)$, where $z^*(S)$ is defined by

$$z^*(S) = f_{3,\xi}(\infty, S), \tag{23}$$

or implicitly from

$$\alpha = F_\xi(\alpha, z^*(S), S). \tag{24}$$

The value $z^*(S)$ is directly related to the behavior of the finite-size correlation length at the critical point, since $\xi(\beta_c; L_\parallel, L_\perp) \approx z^*(S)\, L_\perp$. For finite-temperature phase transitions $z^*(S)$ is finite. By considering the behavior of the FSS functions at $z^*(S)$ we can determine the exponents $\gamma_{\mathcal{O}}/\nu$. Indeed, at the critical point we have

$$\mathcal{O}(\beta_c; L_\parallel, L_\perp) \sim L_\perp^{\gamma_{\mathcal{O}}/\nu}, \tag{25}$$

so that

$$F_{\mathcal{O}}(\alpha, z^*(S), S) = \frac{\mathcal{O}(\beta_c; \alpha L_\parallel, \alpha L_\perp)}{\mathcal{O}(\beta_c; L_\parallel, L_\perp)} = \alpha^{\gamma_{\mathcal{O}}/\nu}, \tag{26}$$

and therefore

$$\frac{\gamma_{\mathcal{O}}}{\nu} = \frac{\log F_{\mathcal{O}}(\alpha, z^*(S), S)}{\log \alpha}. \tag{27}$$

By studying the behavior of $F_\xi(\alpha, z, S)$ in a neighborhood of $z^*(S)$ it is also possible to derive the exponent ν. Using the fact that

$$\frac{\xi(\beta; L_\parallel, L_\perp)}{L_\perp} \approx z^*(S) + a(S)(\beta - \beta_c)\, L_\perp^{1/\nu}, \tag{28}$$

near the critical point, we obtain

$$z \left. \frac{\partial F_\xi(\alpha, z, S)}{\partial z} \right|_{z=z^*(S)} = \alpha(\alpha^{1/\nu} - 1). \tag{29}$$

The above-presented results are valid for an isotropic system. On the other hand, the numerical simulations and the field-theoretical studies predict that the phase transition in the DLG is strongly anisotropic. For example, the scaling form of the critical static two-point function should be

$$\tilde{G}(k_\parallel, k_\perp) \approx \mu^{-2+\eta_\perp} \tilde{G}(\mu^{1+\Delta} k_\parallel, \mu k_\perp), \tag{30}$$

where $\eta_\perp$ is the anomalous dimension of the density field (see ref. 3 for definitions) and Δ is the so-called *anisotropy exponent*.

It is then natural to assume the existence of two correlation lengths $\xi_\perp$, $\xi_\parallel$ which diverge with different exponents $\nu_\perp$ and $\nu_\parallel$ related by[3]

$$\nu_\parallel = (1+\Delta)\, \nu_\perp. \tag{31}$$

These considerations call for an extension of the FSS arguments. A phenomenological approach to FSS for the DLG has been developed,[25] keeping into account the strong anisotropy observed in the transition (for $d=2$ see refs. 14, 15, and 17, for $d=3$ see ref. 16). Following this approach, we assume that all observables have a finite FSS limit for $L_\parallel$, $L_\perp \to \infty$ keeping constant:

- the *anisotropic aspect ratio* $S_\Delta \equiv L_\parallel^{1/(1+\Delta)} / L_\perp$;
- the *FSS parameter* $\xi_{\perp,\infty}(\beta)/L_\perp$ (or equivalently its longitudinal counterpart).

Then, Eq. (21) still holds by using the correct parameters, i.e., by replacing S with S_Δ, ν with $\nu_\perp$, and ξ_∞ with $\xi_{\perp,\infty}$. Analogously, Eq. (22) is recast in the form

$$\frac{\mathcal{O}(\beta; \alpha^{1+\Delta} L_\parallel, \alpha L_\perp)}{\mathcal{O}(\beta; L_\parallel, L_\perp)} = F_{\mathcal{O}} \left(\alpha, \frac{\xi_\perp(\beta; L_\parallel, L_\perp)}{L_\perp}, S_\Delta \right). \tag{32}$$

Equation (32) is the basis for our analysis of the phase transition in the DLG. For the transverse finite-volume correlation length $\xi_\perp$ we use ξ_{13} defined in Section 2.2.

In anisotropic systems the FSS limit must be taken at fixed S_Δ, which in turn requires the knowledge of the exact value of Δ. It is thus important

to understand how we can single out the correct value of Δ from the simulations. First, it should be noticed that observing FSS does not imply that we are using the correct value of Δ.[31] Indeed, note first that Eqs. (21) and (32) still hold for $L_\parallel = \infty$—this corresponds to $S_\Delta = \infty$—i.e., for a geometry $\infty \times L_\perp^{d-1}$ (in two dimensions this is a strip). Then, imagine that we use an incorrect value δ, keeping S_δ fixed in the FSS limit. If $\delta > \Delta$, $L_\parallel$ increases much faster than it should and $S_\Delta \to \infty$. We thus expect to obtain the FSS behavior corresponding to a geometry $\infty \times L_\perp^{d-1}$. Thus, we should be able to observe scaling whenever we use $L_\perp$ as reference length and consider transverse quantities. On the other hand, longitudinal quantities are expected not to scale properly. For instance, $\xi_\parallel / L_\parallel$ should not have a good FSS behavior when plotted vs. $\xi_\perp / L_\perp$. Indeed, at fixed S_Δ we have that $\xi_\parallel \sim L_\parallel \sim L_\perp^{1+\Delta}$. If instead S_δ is fixed and $\delta > \Delta$, $L_\parallel$ increases too fast, so that we expect $\xi_\parallel$ to be controlled by the transverse size only. Thus, $\xi_\parallel$ should increase slower than $L_\parallel$, and thus, at fixed $\xi_\perp / L_\perp$, one should observe $\xi_\parallel / L_\parallel \to 0$. If $\delta < \Delta$ the same argument holds by simply interchanging longitudinal and transverse quantities. This observation provides therefore a method to determine the correct value of Δ. It is the value for which both correlation lengths scale correctly, i.e., $\xi_\parallel \sim L_\parallel$ and $\xi_\perp \sim L_\perp$.

4. FIELD-THEORY DESCRIPTION OF THE DLG

As we explained in Section 2.1, the DLG is a lattice gas model. However, in a neighborhood of the critical point (critical region) we can limit ourselves to consider slowly-varying (in space and time) observables. At criticality the lattice spacing is negligible compared to the length and time scales at which long-range order is established so that it is possible to formulate a description of the system in terms of *mesoscopic* variables. In principle, the dynamics of such variables can be obtained by coarse graining the microscopic system. However, given the difficulty of performing a rigorous coarse-graining procedure, one postulates a continuum field theory that possesses all the symmetries of the microscopic lattice model. By universality the continuum theory should have the same critical behavior of the microscopic one.

Unfortunately, there is at present no consensus on the field theory that describes the critical behavior of the DLG.[10] The theory originally proposed by JSLC[6, 7] has been recently disputed in refs. 8–10 (see also ref. 11), where it is proposed that the DLG at infinite driving field is in the same universality class as the randomly driven lattice gas (RDLG).[18, 19]

[10] The effects of an external drive on the standard Model-B dynamics were also studied in ref. 32.

Both theories agree on the anisotropic nature of the phase transition, but disagree on its origin and make different predictions for the universal quantities.

In the JSLC theory the critical exponents are exactly predicted, and, for $2 \leqslant d \leqslant 5$, they are given by

$$\eta_\perp = 0, \tag{33}$$

$$\nu_\perp = \tfrac{1}{2}, \tag{34}$$

$$\gamma_\perp = 1, \tag{35}$$

$$\beta_\perp = \tfrac{1}{2}, \tag{36}$$

$$\Delta = \tfrac{1}{3}(8-d). \tag{37}$$

In the RDLG model critical exponents are only known up to two loops perturbatively in $\epsilon \equiv 3-d$. Therefore, it is difficult to estimate how much they differ from the JSLC ones. We note that Δ should be quite different in the two theories in two dimensions. In the RDLG we should have $\Delta \approx 1$, since[19] $\Delta = 1-\eta/2$ and we expect η to be small. On the other hand, Eq. (37) gives $\Delta = 2$.

For the JSLC theory, not only do we have exact predictions for the exponents, but we can also compute exactly the transverse structure factor (15). Keeping into account causality[6, 33–35] and the form of the interaction vertex one can see that for $k_\parallel = 0$ there are no loop contributions to the two-point function $\tilde{G}(k)$ (and also to the two-point response function). Thus, for all $2 \leqslant d \leqslant 5$, $\tilde{G}_\perp(k)$ is simply given, in the field-theoretical approach of JSLC, by the tree-level expression

$$\tilde{G}_\perp(k) = \frac{1}{k^2+\tau}, \tag{38}$$

where τ is a squared "bare mass" that vanishes at criticality. Two observations are in order. First, $\tau = bt + O(t^2)$ for $t \equiv (\beta_c - \beta)/\beta_c \to 0$ with b positive constant. Second, the function that appears in Eq. (38) refers to the coarse-grained fields, which, in the critical limit, differ by a finite renormalization from the lattice ones. Thus, for the lattice function we are interested in, in the scaling limit $t \to 0$, $k \to 0$, with k^2/t fixed, we have

$$\tilde{G}_{\perp,\,\mathrm{latt}}(k) = \frac{Z}{k^2+bt}, \tag{39}$$

where Z and b are positive constants.

On the same footing, we can conclude that all correlation functions with vanishing longitudinal momenta behave as in a free theory. In particular, the Binder cumulant defined in Eq. (13) vanishes. It is also important to notice that Eq. (39) implies the exponential decay of

$$G_{\perp,\,\mathrm{latt}}(x_\perp) = \int d^{d-1}k\, e^{ikx_\perp} \tilde{G}_{\perp,\,\mathrm{latt}}(k), \tag{40}$$

which fully justifies our definition of transverse correlation length.

Field-theoretical methods can also be used to determine the FSS behavior of the model. Predictions are easily obtained by following the method applied in equilibrium spin systems (see, e.g., ref. 36, Chap. 36, and references therein). The idea is quite simple. Consider the system in a finite box with periodic boundary conditions. The finite geometry has the only effect of quantizing the momenta. Thus, the perturbative finite-volume correlation functions are obtained by replacing momentum integrals by lattice sums. Ultraviolet divergences are not affected by the presence of the box[37] and thus one can use the infinite-volume renormalization constants. Once the renormalization is carried out, one obtains the geometry-dependent finite-size correlation functions.

The considerations we have presented above for the infinite-volume case apply also in finite volume and thus Eq. (39) holds in this case. Using Eq. (39), in the FSS limit we find

$$\frac{\xi_\perp(\beta; L_\parallel, L_\perp)}{L_\perp} = [(2\pi)^2 + btL_\perp^2]^{-1/2}, \tag{41}$$

valid for $t \to 0$, $L_\parallel, L_\perp \to \infty$ with $tL_\perp^2$ fixed. Although we have not explicitly mentioned S_Δ and such a quantity does not appear in Eq. (41), this expression is expected to be valid only if the FSS limit is taken by keeping S_Δ constant. Taking the limit $L_\perp \to \infty$ we obtain $\xi_{\perp,\infty}(\beta)^2 \approx 1/(bt)$, so that we can write Eq. (41) also in the form

$$\frac{1}{[\xi_\perp(\beta; L_\parallel, L_\perp)]^2} = \frac{1}{\xi_\infty^2(\beta)} + \frac{4\pi^2}{L_\perp^2}. \tag{42}$$

Using Eqs. (42) and (39) we can also compute the scaling functions $F_\xi(\alpha, z, S_\Delta)$ and $F_\chi(\alpha, z, S_\Delta)$ defined in Eq. (32). We obtain

$$F_\xi(\alpha, z, S_\Delta) = [1 - (1 - \alpha^{-2})(2\pi)^2 z^2]^{-1/2}, \tag{43}$$

$$F_\chi(\alpha, z, S_\Delta) = F_\xi^2(\alpha, z, S_\Delta) = [1 - (1 - \alpha^{-2})(2\pi)^2 z^2]^{-1}. \tag{44}$$

Note that these functions do not depend on S_Δ and that

$$z^*(S_\Delta) = \frac{1}{2\pi}. \tag{45}$$

A peculiarity of the JSLC theory is the presence of an operator with renormalization-group dimension $2\sigma = 2(d-2)/3$ that is dangerously irrelevant for $2 < d < 5$ and becomes marginal at $d = 2$. Keeping into account the coupling u associated with the dangerously irrelevant operator, in the JSLC theory we have[6]

$$\begin{aligned}\Gamma_{\tilde{n},n}(\{(q_\parallel, q_\perp)\}, \omega, \tau, u; L_\parallel, L_\perp) &= \ell^{-(d+4+\Delta)+\frac{d+2+\Delta}{2}\tilde{n}+\frac{d-2+\Delta}{2}n} \\ &\times \Gamma_{\tilde{n},n}(\{(\ell^{1+\Delta}q_\parallel, \ell q_\perp)\}, \ell^4\omega, \ell^2\tau, \ell^{-2\sigma}u; \ell^{-1-\Delta}L_\parallel, \ell^{-1}L_\perp),\end{aligned} \tag{46}$$

where $\Gamma_{\tilde{n},n}$ is the one-particle irreducible correlation function of n density fields and $\tilde{n}$ response fields. For the transverse structure factor it implies

$$\tilde{G}_\perp(q_\perp, \tau, u; L_\parallel, L_\perp) = \ell^2 \tilde{G}_\perp(\ell q_\perp, \ell^2\tau, \ell^{-2\sigma}u; \ell^{-1-\Delta}L_\parallel, \ell^{-1}L_\perp). \tag{47}$$

Setting $\ell = L_\perp$ and expanding for $L_\perp \to \infty$ we obtain for $2 < d < 5$

$$\tilde{G}_\perp(q_\perp, \tau, u; L_\parallel, L_\perp) = L_\perp^2 f_2(q_\perp L_\perp, \tau L_\perp^2; S_\Delta)[1 + O(uL_\perp^{-2\sigma})]. \tag{48}$$

Now the leading term is given by Eq. (38), and thus, in the absence of zero mode, which implies $|q_\perp| L_\perp \geqslant 2\pi$, $f_2(q_\perp L_\perp, \tau L_\perp^2; S_\Delta)$ is regular and finite in the whole high-temperature phase. Thus, the dangerously irrelevant coupling can be neglected for all $2 < d < 5$. Note that this argument would not apply to the zero mode if it were present. Indeed, for $q_\perp = 0$, $f_2(0, \tau L_\perp^2; S_\Delta) = 1/\tau L_\perp^2$ which is singular as $\tau \to 0$, giving rise to an anomalous behavior. In App. 6 we discuss this phenomenon in the large-N limit of the $O(N)$ model above the upper critical dimension, i.e., for $d > 4$, showing that no anomalous behavior is observed in the absence of zero mode (in particular the Binder parameter vanishes).[11] Therefore, for $d > 2$, Eqs. (43) and (44) should hold without changes. For $d = 2$ the operator becomes marginal ($\sigma = 0$) and therefore we expect logarithmic corrections to the formulae previously computed. In the absence of any prediction, we will neglect these logarithmic violations. As it has been observed in

[11] Even in the absence of zero mode it is still possible to observe anomalous scaling by performing a noncanonical scaling limit. One should consider $\tau \to 0$, $L_\perp \to 0$ with $\tau L_\perp^2 + 4\pi^2 \to 0$ at the same time. See ref. 26 for a discussion in the N-vector model.

previous numerical studies, if present, they are small.[14] As we will discuss, this is confirmed by our numerical results.

Finally, we wish to compute the behavior of the Binder parameter keeping into account the presence of the dangerously irrelevant operator. Considering the connected static four-point correlation function for vanishing parallel momenta, Eq. (46) implies

$$\tilde{G}^{(4)}(\{(0, q_\perp)\}, \tau, u; L_\parallel, L_\perp) = \ell^{d+4+\Delta}\tilde{G}^{(4)}(\{(0, \ell q_\perp)\}, \ell^2\tau, \ell^{-2\sigma}u; \ell^{-1-\Delta}L_\parallel, \ell^{-1}L_\perp). \tag{49}$$

Now $\tilde{G}^{(4)}$ is of order u, and therefore, setting $\ell = L_\perp$, $q_\perp = \pm\bar{q}$ with $|\bar{q}| = 2\pi/L_\perp$ as in the definition of the Binder parameter, cf. Eq. (13), we obtain

$$\tilde{G}^{(4)}(\{(0, \pm\bar{q})\}, \tau, u; L_\parallel, L_\perp) = uL_\perp^8 f_4(\tau L_\perp^2, S_\Delta)[1 + O(uL_\perp^{-2\sigma})]. \tag{50}$$

In Appendix B we have verified this equation to first order in perturbation theory, proving also that $f_4(0, S_\Delta) \neq 0$. It follows that the Binder parameter behaves as

$$\begin{aligned} g(\beta; L_\parallel, L_\perp) &= \frac{uL_\perp^{5-d}}{L_\parallel} f_4(\tau L_\perp^2, S_\Delta)(4\pi^2 + \tau L_\perp^2)^2\,[1 + O(uL_\perp^{-2\sigma})] \\ &= uL_\perp^{-2\sigma} f_g(\tau L_\perp^2, S_\Delta)[1 + O(uL_\perp^{-2\sigma})], \end{aligned} \tag{51}$$

with $f_g(0, S_\Delta) \neq 0$. Therefore, for all $2 < d < 5$ the Binder parameter vanishes, in spite of the presence of the dangerously irrelevant operator. In $d = 2$ we expect logarithmic corrections. Note again that $g(\beta_c; L_\parallel, L_\perp)$ vanishes as $L_\perp \to \infty$ because $f_2(2\pi, 0; S_\Delta) \neq 0$, a consequence of the fact that the Binder parameter we use here is defined at nonvanishing momenta.

Finally, we wish to discuss the distribution function of the order parameter $\psi \equiv \phi(\mathbf{k}_{0,1})$ in the JSLC theory. For $\beta \to \beta_c$ and $L_\parallel$, $L_\perp \to \infty$, such a quantity has a Gaussian distribution, i.e.,

$$N \exp\left(-\frac{|\psi|^2}{L_\parallel L_\perp^{d-1}\chi_\perp}\right) d\psi\, d\psi^*, \tag{52}$$

where N is a normalization factor, and indeed the Binder parameter vanishes in this limit. Since the dangerously irrelevant operator is truly irrelevant, such a distribution is also valid at the critical point and in the FSS limit, allowing the computation of the distribution function of the magnetization. We obtain

$$m^2 = \frac{\pi}{4}\frac{\chi_\perp}{L_\parallel L_\perp^{d-1}}, \tag{53}$$

with corrections of order $L_\perp^{-2\sigma}$ (logarithms in $d = 2$). Then, we obtain

$$F_m(\alpha, z, S_\Delta) = \frac{1}{\alpha^{(d+\Delta)/2}} F_\chi(\alpha, z, S_\Delta)^{1/2}, \tag{54}$$

with logarithmic corrections in $d = 2$.

5. NUMERICAL SIMULATION

5.1. Setup

In order to study the critical behavior of the DLG in two dimensions, we perform an extensive Monte Carlo simulation. We use the dynamics described in Section 2.1 with Metropolis rates, i.e., we set

$$w(x) = \min(1, e^{-x}). \tag{55}$$

Simulations are performed at infinite driving field. Therefore, forward (backward) jumps in the direction of the field are always accepted (rejected).

The dynamics of the DLG is diffusive and the dynamic critical exponent associated with transverse fluctuations, which represent the slowest modes of the system, is expected to be close to 4 both in the JSLC and in the RDLG models. In the JSLC theory[6] $z_\perp = 4$ exactly. Thus, it is important to have an efficient implementation of the Monte Carlo algorithm in order to cope with the severe critical slowing down.

We use a multi-spin coding technique, evolving simultaneously N_{multi} independent configurations. We took particular care in optimizing the value N_{multi}. On Pentium and PowerPC processors—the computers we used in our simulations—we observed a nonmonotonic behavior of the speed with N_{multi}. For instance, on a Pentium processor, we reach a speed of $1.3 \cdot 10^8$ spin-flips/sec for $N_{\text{multi}} = 32$ and $2.7 \cdot 10^8$ for $N_{\text{multi}} = 128$. The speed drops to $2.0 \cdot 10^8$ for $N_{\text{multi}} = 192$ and then increases again, reaching $3.8 \cdot 10^8$ for $N_{\text{multi}} = 960$. However, by increasing N_{multi} we increase the memory and disk requirements so that we used $N_{\text{multi}} = 128$ as a good compromise.

For the pseudo-random numbers we use the Parisi–Rapuano congruential generator, a 32-bit shift-register generator based on

$$a_n = (a_{n-24} + a_{n-55}) \text{ XOR } a_{n-61}, \tag{56}$$

where a_n is an unsigned 32-bit integer.

The main purpose of our work is to test the theoretical predictions of the JSLC field-theoretical model discussed in Section 4. It predicts $\Delta = 2$ and therefore we have performed simulations on a set of lattices with

$L_\parallel/L_\perp^3$ constant. We considered the following values of $(L_\parallel, L_\perp)$: (21, 14), (32, 16), (46, 18), (64, 20), (88, 22), (110, 24), (168, 28), (216, 30), (262, 32), (373, 36), (512, 40), (592, 42), (681, 44), (778, 46), (884, 48). It is easy to verify that $S_2 \approx 0.200$ (more precisely $0.197 \leqslant S_2 \leqslant 0.202$ for $L_\perp \leqslant 28$ and $0.19992 \leqslant S_2 \leqslant 1/5$ for $L_\perp \geqslant 30$). We considered several values of β: 0.28, 0.29, 0.3, 0.305, 0.3075, 0.31, 0.3105, 0.311, 0.31125, 0.3115, 0.31175, 0.312. As we shall see below, all lie in the disordered phase, albeit very near to the critical point. For a few values of β we have also performed simulations for different values of $(L_\parallel, L_\perp)$. We have considered a sequence of lattices with $S_2 \approx 0.300$ and $S_2 \approx 0.100$ [the largest lattice has $(L_\parallel, L_\perp) = (1350, 30)$, (414, 48) respectively] and a sequence with $\Delta = 1$ and $S_1 \approx 0.106$ [the largest lattice has $(L_\parallel, L_\perp) = (245, 48)$]. The results for $\Delta = 2$ and $S_2 \approx 0.200$ are presented in Table I.

It is very important to be sure that the system has reached the steady-state distribution before sampling. Metastable configurations in which the system is trapped for times much longer than typical relaxation times in the steady state are a dangerous source of bias. In the DLG, configurations with multiple stripes aligned with the external field are very long-lived and may persist for times of the order of a typical simulation run. To avoid them, we started the simulations for the largest systems from suitably rescaled thermalized configurations of smaller lattices at the same temperature and value of S_Δ.

We have performed a detailed study of the dynamic correlations. For $\beta = 0.312$, the value of β that is nearest to β_c, we compute the autocorrelation time τ_χ for the susceptibility $\chi_\perp$, which is expected to have a significant overlap with the slowest modes of the system. The results are reported in Table II. The autocorrelation times are expressed in sweeps, where a sweep is conventionally defined as the number of proposed moves equal to the volume of the lattice. It is easy to verify that $\tau_\chi \sim L_\perp^4$ as expected. For each β and lattice size we always make at least $3 \cdot 10^7$ sweeps, so that our runs are at least, but in most of the cases much longer than, approximately $10^3 \tau_\chi$.

The statistical variance of the observables is estimated by using the jackknife method.[38] To take into account the correlations of the samples, we used a blocking technique in the jackknife analysis, using blocks of 256×10^3 sweeps. They are much longer than typical autocorrelation times and thus different blocks are statistically independent.

5.2. Results

First, we check that the correlation length $\xi_\perp(\beta; L_\parallel, L_\perp)$ has a good thermodynamic limit, independent of the aspect ratio, i.e., that, for $\beta < \beta_c$, $\xi_\perp(\beta; L_\parallel, L_\perp)$ has a finite limit when $L_\parallel, L_\perp \to \infty$ in an arbitrary way.

Table I. The Results of Our Simulations with $\Delta = 2$ and $S_2 \approx 0.200$. Here $A \equiv \xi_\perp^2/\chi_\perp$

$L_\parallel$	$L_\perp$	$\xi_\perp$	$\chi_\perp$	A	m	g	$\xi_\parallel$
				$\beta = 0.28$			
32	16	1.6191(18)	10.758(12)	0.24368(40)	0.130291(73)	0.19471(80)	1.5953(65)
46	18	1.6939(19)	11.782(13)	0.24353(42)	0.106822(60)	0.14899(76)	2.5022(91)
64	20	1.7486(24)	12.577(15)	0.24312(52)	0.088528(55)	0.11355(89)	3.641(10)
88	22	1.7952(23)	13.221(16)	0.24375(45)	0.073648(45)	0.08358(94)	5.122(12)
110	24	1.8295(27)	13.731(17)	0.24375(55)	0.064195(40)	0.0663(11)	6.346(13)
168	28	1.8838(33)	14.568(22)	0.24359(60)	0.049452(37)	0.0416(11)	9.453(23)
262	32	1.9130(38)	15.109(23)	0.24221(70)	0.037688(30)	0.0277(11)	13.582(41)
373	36	1.9339(50)	15.484(28)	0.24155(93)	0.030126(27)	0.0167(13)	17.804(73)
512	40	1.9589(64)	15.839(38)	0.2423(12)	0.024660(29)	0.0089(24)	22.22(13)
				$\beta = 0.29$			
32	16	1.8263(17)	13.231(13)	0.25208(39)	0.145232(73)	0.25367(72)	1.7096(61)
46	18	1.9385(20)	14.892(18)	0.25235(37)	0.120651(76)	0.20415(84)	2.6886(74)
64	20	2.0284(26)	16.334(19)	0.25189(49)	0.101281(61)	0.16350(80)	3.9684(87)
88	22	2.1010(25)	17.559(23)	0.25139(41)	0.085143(56)	0.12623(83)	5.625(10)
110	24	2.1626(26)	18.572(24)	0.25184(41)	0.074864(49)	0.10536(88)	7.064(12)
168	28	2.2486(38)	20.138(33)	0.25108(56)	0.058257(49)	0.0701(11)	10.627(18)
262	32	2.3090(40)	21.315(37)	0.25011(56)	0.044811(40)	0.0437(13)	15.740(35)
373	36	2.3518(49)	22.110(44)	0.25016(66)	0.036028(36)	0.0285(14)	21.017(54)
512	40	2.387(14)	22.84(10)	0.2494(21)	0.029636(61)	0.0165(55)	27.09(49)
				$\beta = 0.30$			
32	16	2.0810(19)	16.654(18)	0.26003(20)	0.16414(12)	0.3287(11)	1.8128(99)
46	18	2.2599(26)	19.612(20)	0.26040(55)	0.139479(84)	0.2857(11)	2.8963(90)
64	20	2.4111(19)	22.351(29)	0.26009(50)	0.119294(98)	0.2426(13)	4.3016(32)
88	22	2.5570(29)	25.083(30)	0.26066(45)	0.102430(75)	0.20601(64)	6.202(16)
110	24	2.6604(17)	27.218(18)	0.26004(21)	0.091161(32)	0.17936(56)	7.8399(71)
168	28	2.8383(41)	31.017(47)	0.25972(43)	0.072636(58)	0.13168(89)	11.964(14)
262	32	2.9828(34)	34.254(60)	0.25974(33)	0.057022(57)	0.0952(16)	18.223(30)
373	36	3.0875(46)	36.748(72)	0.25942(34)	0.046562(47)	0.0643(12)	24.984(81)
512	40	3.1673(69)	38.735(99)	0.25899(53)	0.038667(45)	0.0487(26)	32.511(60)
				$\beta = 0.3025$			
32	16	2.1529(18)	17.656(16)	0.26252(34)	0.169306(83)	0.34838(66)	1.8477(56)
46	18	2.3538(21)	21.087(22)	0.26274(33)	0.144925(78)	0.30826(63)	2.9442(74)
64	20	2.5344(27)	24.444(31)	0.26276(35)	0.125037(84)	0.26921(72)	4.4080(77)
88	22	2.6955(29)	27.681(36)	0.26249(38)	0.107824(73)	0.23164(74)	6.3251(94)
110	24	2.8283(30)	30.490(40)	0.26235(40)	0.096697(67)	0.20661(81)	8.033(11)
168	28	3.0548(37)	35.567(58)	0.26238(41)	0.077917(66)	0.1559(11)	12.367(16)
262	32	3.2340(55)	39.948(89)	0.26181(44)	0.061649(71)	0.1127(14)	18.913(30)
373	36	3.3720(64)	43.30(11)	0.26258(45)	0.050597(68)	0.0819(16)	26.068(50)
512	40	3.4664(82)	45.92(14)	0.26170(58)	0.042138(63)	0.0598(23)	34.334(90)

Table I. ***(Continued)***

$L_\parallel$	$L_\perp$	$\xi_\perp$	$\chi_\perp$	A	m	g	$\xi_\parallel$
				$\beta = 0.3050$			
32	16	2.2299(16)	18.781(16)	0.26476(24)	0.175010(84)		
46	18	2.4605(22)	22.815(26)	0.26534(26)	0.151172(96)		
64	20	2.6633(27)	26.749(38)	0.26517(27)	0.13114(10)		
88	22	2.8588(35)	30.793(54)	0.26541(29)	0.11403(11)		
110	24	3.0259(43)	34.462(70)	0.26570(29)	0.10308(11)		
168	28	3.3077(62)	41.22(11)	0.26543(36)	0.08412(12)		
216	30	3.4114(70)	44.06(13)	0.26415(36)	0.07390(12)		
256	32	3.5286(85)	47.07(17)	0.26450(42)	0.06786(13)		
365	36	3.710(11)	52.05(22)	0.26442(50)	0.05621(12)		
500	40	3.888(14)	56.95(29)	0.26548(64)	0.04759(13)		
592	42	3.914(16)	57.93(31)	0.26443(99)	0.04298(12)	0.0714(39)	41.03(19)
681	44	3.979(15)	60.18(30)	0.26308(84)	0.039892(98)	0.0653(30)	46.27(16)
778	46	4.038(10)	61.62(20)	0.26462(57)	0.036916(61)	0.0589(20)	51.86(14)
884	48	4.0554(99)	62.51(19)	0.26310(58)	0.034121(55)	0.0483(24)	57.63(16)
				$\beta = 0.3075$			
32	16	2.3093(21)	19.992(18)	0.26676(35)	0.181034(88)	0.39515(57)	1.9069(49)
46	18	2.5687(19)	24.682(23)	0.26733(32)	0.157657(78)	0.36309(69)	3.0624(65)
64	20	2.8141(24)	29.501(31)	0.26844(33)	0.138181(79)	0.33179(70)	4.5961(80)
88	22	3.0400(30)	34.533(43)	0.26762(32)	0.121188(79)	0.29934(68)	6.6479(79)
168	28	3.6017(45)	48.397(93)	0.26804(31)	0.091505(93)	0.2356(11)	13.145(14)
262	32	3.9228(68)	57.37(14)	0.26825(43)	0.074304(94)	0.1859(14)	20.397(27)
373	36	4.1764(87)	65.23(18)	0.26740(45)	0.062411(92)	0.1485(16)	28.500(45)
512	40	4.374(10)	71.66(24)	0.26701(48)	0.052849(94)	0.1167(24)	38.117(78)
681	44	4.549(14)	77.60(34)	0.26669(54)	0.04540(10)	0.0950(21)	48.88(12)
				$\beta = 0.31$			
32	16	2.3975(28)	21.392(31)	0.26870(25)	0.18784(15)	0.42136(99)	1.9320(82)
46	18	2.6893(22)	26.803(21)	0.26983(48)	0.164882(77)	0.39503(46)	3.1211(84)
64	20	2.9691(13)	32.596(27)	0.27044(27)	0.145826(79)	0.36797(77)	4.6893(89)
88	22	3.2437(43)	39.005(63)	0.26975(63)	0.12933(12)	0.3399(14)	6.7983(51)
110	24	3.4866(24)	44.941(38)	0.27049(21)	0.118671(53)	0.32316(66)	8.6928(80)
168	28	3.9556(44)	57.703(84)	0.27116(28)	0.100412(81)	0.2893(11)	13.564(13)
262	32	4.3976(58)	71.31(12)	0.27119(33)	0.083257(82)	0.2425(15)	21.143(30)
373	36	4.7836(81)	84.43(20)	0.27101(36)	0.071388(92)	0.2109(18)	29.947(46)
512	40	5.112(12)	96.54(34)	0.27073(41)	0.06163(12)	0.1760(23)	40.289(97)

Table I. ***(Continued)***

$L_\parallel$	$L_\perp$	$\xi_\perp$	$\chi_\perp$	A	m	g	$\xi_\parallel$
				$\beta = 0.3105$			
32	16	2.4141(18)	21.584(17)	0.27000(31)	0.188709(78)	0.42424(50)	1.9437(49)
46	18	2.7082(23)	27.167(24)	0.26996(34)	0.166028(80)	0.39866(62)	3.1332(61)
64	20	3.0040(30)	33.295(35)	0.27104(40)	0.147436(82)	0.37382(59)	4.7005(70)
88	22	3.2910(33)	39.952(49)	0.27109(35)	0.130987(88)	0.34836(80)	6.8253(92)
110	24	3.5446(38)	46.274(61)	0.27151(37)	0.120523(85)	0.33253(72)	8.749(11)
168	28	4.0443(58)	60.03(12)	0.27247(37)	0.10250(11)	0.2993(12)	13.658(15)
262	32	4.5097(78)	74.75(19)	0.27205(37)	0.08534(12)	0.2559(13)	21.358(23)
373	36	4.940(11)	89.79(30)	0.27177(41)	0.07372(13)	0.2281(18)	30.152(49)
512	40	5.291(13)	103.04(38)	0.27166(45)	0.06374(13)	0.1934(20)	40.584(81)
				$\beta = 0.3110$			
32	16	2.4295(20)	21.876(18)	0.26982(35)	0.190095(85)	0.42942(53)	1.9526(50)
46	18	2.7330(23)	27.666(25)	0.26998(34)	0.167675(85)	0.40611(63)	3.1384(68)
64	20	3.0375(31)	34.004(36)	0.27133(39)	0.149149(86)	0.38293(61)	4.7344(75)
88	22	3.3367(30)	40.949(49)	0.27189(36)	0.132722(85)	0.35717(70)	6.8476(85)
110	24	3.6087(35)	47.810(61)	0.27239(36)	0.122655(85)	0.34509(79)	8.787(10)
168	28	4.1255(52)	62.29(11)	0.27324(33)	0.10453(10)	0.3117(11)	13.767(15)
262	32	4.6328(72)	78.78(19)	0.27243(35)	0.08778(11)	0.2775(12)	21.587(23)
373	36	5.094(12)	95.09(33)	0.27294(44)	0.07597(14)	0.2445(20)	30.390(43)
512	40	5.497(12)	110.66(39)	0.27303(38)	0.06615(13)	0.2101(22)	41.149(65)
592	42	5.675(10)	118.34(32)	0.27217(33)	0.062069(87)	0.2028(15)	47.288(60)
681	44	5.900(14)	127.52(47)	0.27299(37)	0.05864(11)	0.1943(19)	53.826(94)
778	46	6.060(21)	134.56(72)	0.27292(51)	0.05503(16)	0.1776(32)	61.22(17)
884	48	6.176(25)	140.72(88)	0.27105(64)	0.05165(17)	0.1672(32)	69.04(20)
				$\beta = 0.31125$			
32	16	2.4391(21)	22.020(21)	0.27017(34)	0.190759(98)	0.43198(51)	1.9496(46)
46	18	2.7438(24)	27.858(25)	0.27025(36)	0.168324(83)	0.40925(54)	3.1504(59)
64	20	3.0473(30)	34.278(36)	0.27090(40)	0.149801(87)	0.38624(68)	4.7501(71)
88	22	3.3586(35)	41.500(52)	0.27182(35)	0.133692(89)	0.36231(68)	6.880(11)
110	24	3.6414(40)	48.512(68)	0.27334(33)	0.123605(96)	0.34876(90)	8.7956(94)
168	28	4.1695(60)	63.68(13)	0.27298(39)	0.10579(11)	0.3197(11)	13.791(15)
262	32	4.6869(85)	80.48(23)	0.27293(37)	0.08872(13)	0.2777(13)	21.586(26)
373	36	5.172(11)	97.82(33)	0.27350(41)	0.07711(14)	0.2516(17)	30.574(43)
512	40	5.604(19)	115.01(60)	0.27304(62)	0.06757(18)	0.2286(28)	41.61(13)

Table I. ***(Continued)***

$L_\parallel$	$L_\perp$	$\xi_\perp$	$\chi_\perp$	A	m	g	$\xi_\parallel$
				$\beta = 0.3115$			
32	16	2.4499(21)	22.206(20)	0.27029(35)	0.191660(94)	0.43570(56)	1.9444(47)
46	18	2.7630(23)	28.101(26)	0.27166(33)	0.169113(85)	0.41200(53)	3.1561(62)
64	20	3.0710(26)	34.685(33)	0.27190(34)	0.150740(77)	0.38977(61)	4.7504(72)
88	22	3.3783(39)	42.010(63)	0.27167(36)	0.13457(11)	0.36717(79)	6.894(10)
110	24	3.6678(42)	49.176(70)	0.27356(39)	0.124528(95)	0.35446(75)	8.8076(88)
168	28	4.2136(58)	64.79(12)	0.27404(38)	0.10677(10)	0.32546(96)	13.840(14)
262	32	4.7588(76)	82.70(20)	0.27383(39)	0.09004(12)	0.2897(13)	21.687(26)
373	36	5.2512(90)	100.80(27)	0.27356(32)	0.07832(11)	0.2583(15)	30.613(44)
512	40	5.698(13)	118.80(42)	0.27327(43)	0.06871(13)	0.2344(20)	41.721(66)
				$\beta = 0.3118$			
32	16	2.4574(22)	22.305(18)	0.27073(38)	0.192139(82)	0.43817(50)	1.9559(55)
46	18	2.7764(21)	28.383(23)	0.27159(31)	0.170033(76)	0.41621(51)	3.1652(61)
64	20	3.0867(27)	35.021(38)	0.27207(32)	0.151519(88)	0.39259(56)	4.7673(68)
88	22	3.4079(36)	42.577(56)	0.27277(35)	0.135525(97)	0.37079(73)	6.9033(91)
110	24	3.6859(45)	49.781(77)	0.27291(38)	0.12533(11)	0.35856(88)	8.846(11)
168	28	4.2503(57)	66.04(13)	0.27352(36)	0.10787(11)	0.3322(12)	13.855(15)
262	32	4.8231(79)	84.93(21)	0.27390(39)	0.09131(12)	0.2979(12)	21.773(29)
373	36	5.3518(97)	104.56(30)	0.27392(40)	0.07985(12)	0.2702(18)	30.811(53)
512	40	5.824(15)	123.75(52)	0.27406(42)	0.07015(16)	0.2419(23)	41.981(78)
				$\beta = 0.312$			
32	16	2.4678(20)	22.462(19)	0.27113(34)	0.192845(85)	0.43929(51)	1.9516(55)
46	18	2.7878(22)	28.602(24)	0.27173(34)	0.170722(77)	0.41788(58)	3.1652(62)
64	20	3.1094(26)	35.444(36)	0.27279(34)	0.152516(82)	0.39803(57)	4.7690(69)
88	22	3.4340(31)	43.148(50)	0.27331(33)	0.136530(86)	0.37673(70)	6.9430(85)
110	24	3.7134(37)	50.531(64)	0.27289(37)	0.126343(86)	0.36395(73)	8.879(11)
168	28	4.2984(63)	67.50(13)	0.27372(39)	0.10914(11)	0.3402(11)	13.924(14)
262	32	4.8875(75)	87.18(20)	0.27400(35)	0.09258(11)	0.3047(14)	21.838(24)
373	36	5.452(11)	107.89(34)	0.27552(39)	0.08121(14)	0.2824(19)	30.973(50)
512	40	5.947(17)	128.62(60)	0.27501(50)	0.07164(18)	0.2575(23)	42.297(66)
592	42	6.211(12)	140.35(42)	0.27490(28)	0.06784(11)	0.2466(17)	48.474(63)
681	44	6.457(19)	151.99(71)	0.27428(46)	0.06427(16)	0.2389(26)	55.32(11)
778	46	6.718(37)	163.8(1.5)	0.27547(67)	0.06097(30)	0.2271(49)	62.87(24)
884	48	6.967(41)	176.7(1.8)	0.27476(44)	0.05773(21)	0.2143(29)	70.94(14)

Table II. Integrated Autocorrelation Times τ_χ (Expressed in Sweeps) for the Susceptibility for $\beta = 0.312$

$L_\perp$	τ_χ
28	2182(82)
32	3934(190)
36	6044(359)
40	9306(738)
42	11040(615)
44	12790(986)
46	21190(3218)
48	20460(1115)

Instead of $\xi_\perp(\beta; L_\parallel, L_\perp)$ we consider (the reason of this definition will become clear below)

$$\tau(\beta; L_\parallel, L_\perp) \equiv \frac{1}{\xi_\perp^2(\beta; L_\parallel, L_\perp)} - \frac{4\pi^2}{L_\perp^2}. \tag{57}$$

Of course, if $\xi_\perp(\beta; L_\parallel, L_\perp)$ has a good thermodynamic limit, also $\tau(\beta; L_\parallel, L_\perp)$ has a finite limit and

$$\lim_{L_\parallel, L_\perp \to \infty} \tau(\beta; L_\parallel, L_\perp) = \frac{1}{\xi_{\perp,\infty}^2(\beta)}. \tag{58}$$

In Fig. 1 we show $\tau(\beta; L_\parallel, L_\perp)$ for four values of β and two different sequences of lattice sizes, one with $S_2 \approx 0.200$ and the other one with $S_1 \approx 0.106$. The numerical results show that $\tau(\beta; L_\parallel, L_\perp)$ has a finite infinite-volume limit, which is reached from below using the data with fixed S_2 and from above using the data with fixed S_1. The corrections to Eq. (58) are not clear. In equilibrium systems the second-moment correlation length converges to $\xi_{\perp,\infty}(\beta)$ with corrections that decrease as $1/L_\parallel^2$, $1/L_\perp^2$, although in many cases, with an appropriate finite-volume definition, such corrections are so small that an apparent exponential convergence is observed.[39] These corrections can be easily related to the behavior of $\tilde{G}_{\perp,\infty}(q)$ in infinite volume. Indeed, $\tilde{G}_\perp(q; L_\parallel, L_\perp)$ converges to $\tilde{G}_{\perp,\infty}(q)$ exponentially and thus we obtain for $\xi_\perp \equiv \xi_{13}$ defined in Eq. (16)

$$\xi_\perp^2(\beta; L_\parallel, L_\perp) = \xi_{\perp,\infty}^2 \left[1 + \frac{\xi_{\perp,\infty}^2}{L_\perp^2} \left(-4\pi^2 + \frac{10\pi^2}{3\xi_{\perp,\infty}^2} + \frac{20\pi^2 c(\beta)}{\xi_{\perp,\infty}^2} \right) + O(L_\perp^{-4}) \right], \tag{59}$$

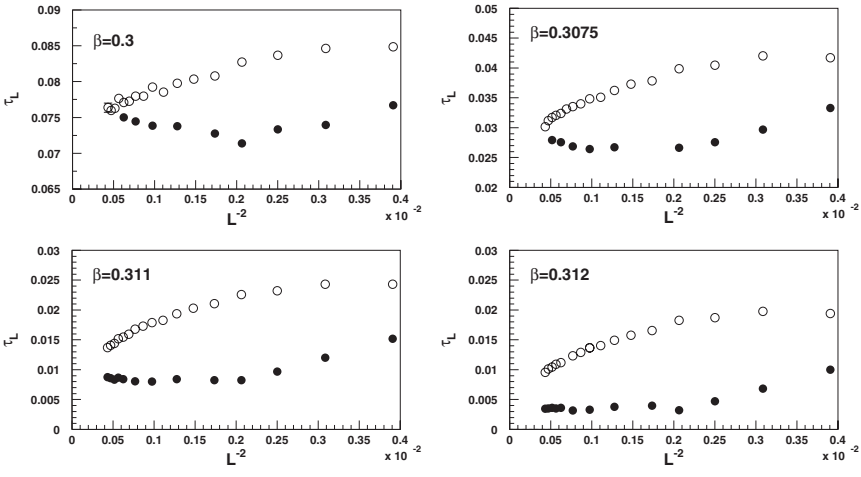

Fig. 1. $\tau_L \equiv \tau(\beta; L_\parallel, L_\perp)$ for different lattices as a function of $L^{-2} \equiv L_\perp^{-2}$. Filled (respectively empty) points refer to lattices with aspect ratio S_2 (respectively S_1) fixed. Here $S_2 \approx 0.200$, $S_1 \approx 0.106$. Errors are smaller than the size of the points.

where

$$c(\beta) = \left. \frac{\partial^2 \tilde{G}^{-1}_{\perp,\infty}(q)/\partial(q^2)^2}{\partial \tilde{G}^{-1}_{\perp,\infty}(q)/\partial q^2} \right|_{q=0}. \tag{60}$$

This expression is valid for any β, not only near the critical point. It shows that corrections vanish as $L_\perp^{-2}$, although it does not allow to compute them, since $c(\beta)$, which for scaling reasons is expected to scale as $\xi^2_{\perp,\infty}$ as $\beta \to \beta_c$, is unknown. In the DLG case, we do not know what are the finite-volume corrections to the structure factor, but it is still reasonable to conjecture that corrections to $\xi_\perp$ vanish as $L_\perp^{-2}$. The results reported in Fig. 1 confirm this behavior. One apparently observes a $L_\perp^{-2}$ correction, especially for the lattices with fixed S_1. It is interesting to observe that, considering the data with fixed S_2, the finite-size corrections decrease as $\beta \to \beta_c$. This is due to our specific definition of $\tau(\beta; L_\parallel, L_\perp)$ and is the motivation for this choice. Indeed, Eq. (42) implies

$$\tau(\beta; L_\parallel, L_\perp) \approx \frac{1}{\xi^2_{\perp,\infty}(\beta)} + o(L_\perp^{-2}), \tag{61}$$

i.e., corrections vanish faster than $L_\perp^{-2}$, in the FSS limit at fixed S_2. The data in Fig. 1 confirm this behavior and thus support the JSLC prediction (42).

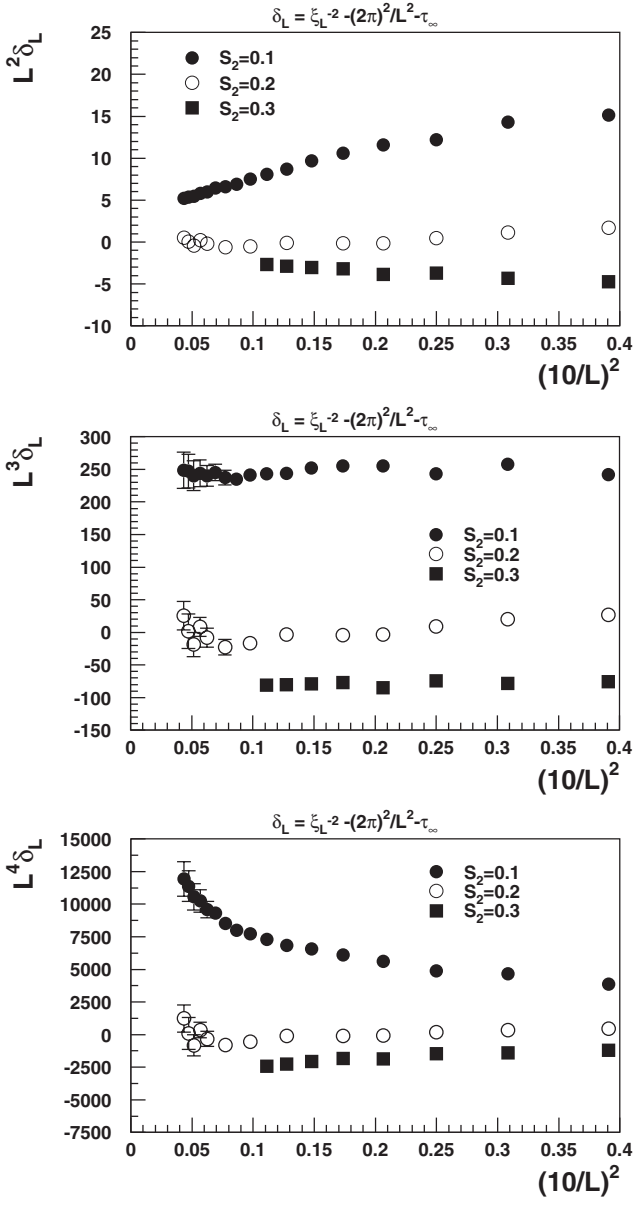

Fig. 2. $L_\perp^a \delta(\beta; L_\parallel, L_\perp)$ for different lattices and S_2 as a function of $L_\perp^{-2}$. Here $a = 2, 3, 4$.

For $\beta = 0.311$ we have performed a more detailed check by comparing results for three different values of S_2. We define

$$\delta(\beta; L_\parallel, L_\perp) \equiv \tau(\beta; L_\parallel, L_\perp) - \tau_\infty(\beta), \tag{62}$$

where $\tau_\infty(\beta)$ is the extrapolated value of $\tau(\beta; L_\parallel, L_\perp)$ for $L_\perp = \infty$. If Eq. (61) holds, such a quantity vanishes as $L_\perp^{-2-\omega}$ for $L_\perp \to \infty$, where $\omega > 0$ is a correction-to-scaling exponent. In Fig. 2 we report $L_\perp^a \delta_L(\beta; L_\parallel, L_\perp)$ for three different values of a. For $a = 2+\omega$, points with constant S_2 should lie on an approximately horizontal line. From Fig. 2 we obtain $\omega \approx 1$, i.e., $\tau(\beta; L_\parallel, L_\perp) = \tau_\infty(\beta) + O(L_\perp^{-3})$ for β close to β_c.

We wish now to perform a detailed FSS analysis comparing the numerical data with the predictions (43) and (44). First, we consider the correlation length using $\alpha = 2$. In Fig. 3 we report our results for $\xi_\perp(\beta; 8L_\parallel, 2L_\perp)/\xi_\perp(\beta; L_\parallel, L_\perp)$ vs. $\xi_\perp(\beta; L_\parallel, L_\perp)/L_\perp$. The solid line is the theoretical prediction (43). It is clear that, as the size of the lattice increases, the points converge towards the theoretical line. We would like

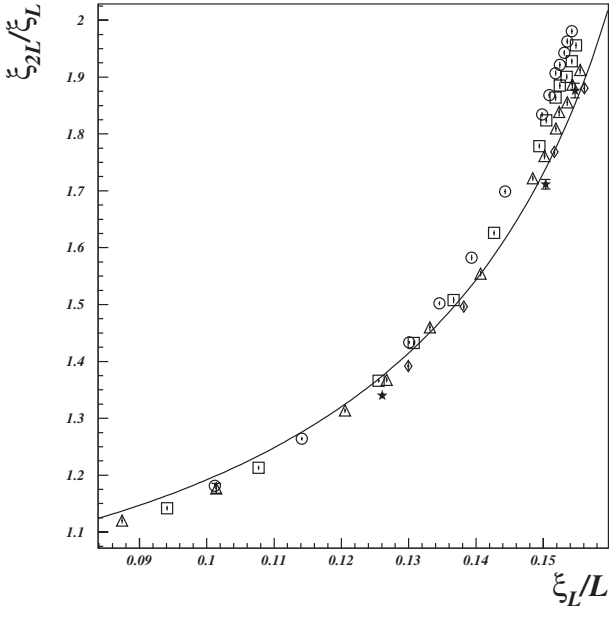

Fig. 3. FSS plot for the transverse correlation length $\xi_\perp$ with $\alpha = 2$ and $S_2 \approx 0.200$. Here $\xi_L = \xi_\perp(\beta; L_\parallel, L_\perp)$, $\xi_{2L} = \xi_\perp(\beta; 8L_\parallel, 2L_\perp)$, $L = L_\perp$. Different symbols correspond to different lattices sizes: $L =$ 16 (○), 18 (□), 20 (△), 22 (◇), 24 (★). The line is the theoretical prediction $F_\xi(2, \xi_L/L, S_2)$, cf. Eq. (43).

to emphasize that in this plot *there are no tunable parameters*. Thus, the observed collapse is very remarkable. To get rid of the small corrections to FSS that are still present, in Fig. 4 we present the same data using on the horizontal axis $\xi_\perp(\beta; 8L_\parallel, 2L_\perp)/(2L_\perp)$. By using the values of $\xi_\perp$ corresponding to the larger lattice, scaling corrections are systematically reduced. Note that the very good agreement between theory and numerical data gives $\nu_\perp = 1/2$. Indeed, using Eq. (43) and Eq. (29) we obtain the mean-field value for the exponent $\nu_\perp$.

Next, we checked the FSS behavior of the susceptibility. In Fig. 5 we report our numerical data together with the theoretical prediction (44). Again, we observe a very good agreement. This result immediately implies $\gamma_\perp = 1$, cf. Eq. (27).

In Fig. 6 we present the same plot for the magnetization. The results are in reasonable agreement with the theoretical prediction (54), although in the region of small $\xi_\perp(\beta; L_\parallel, L_\perp)/L_\perp$ one can see some deviations. As we discuss below, such deviations can be interpreted as corrections to scaling, that in our case decay quite slowly, probably as an inverse power of

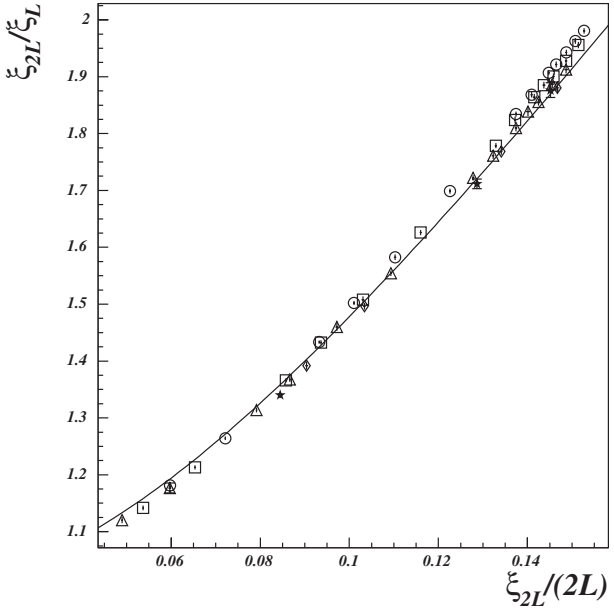

Fig. 4. FSS plot for the transverse correlation length analogous to that presented in Fig. 3. Here we plot the data vs. $\xi_{2L}/(2L) = \xi_\perp(\beta; 8L_\parallel, 2L_\perp)/(2L_\perp)$. Symbols are defined as in Fig. 3. The line is the theoretical prediction.

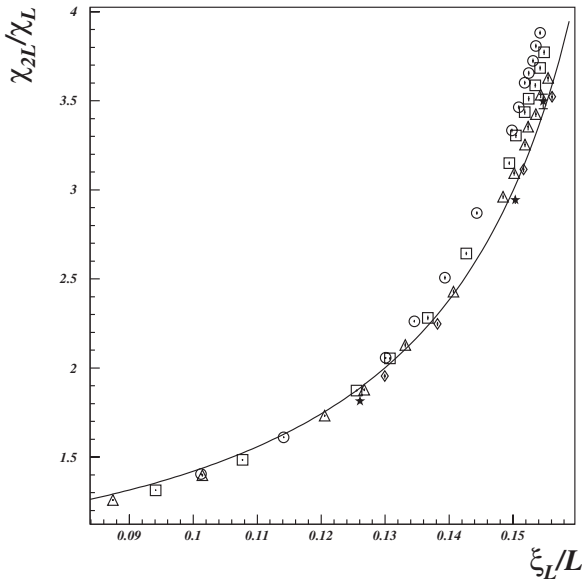

Fig. 5. FSS plot for $\chi_\perp$. Symbols are defined as in Fig. 3. The solid line is the theoretical prediction, cf. Eq. (44).

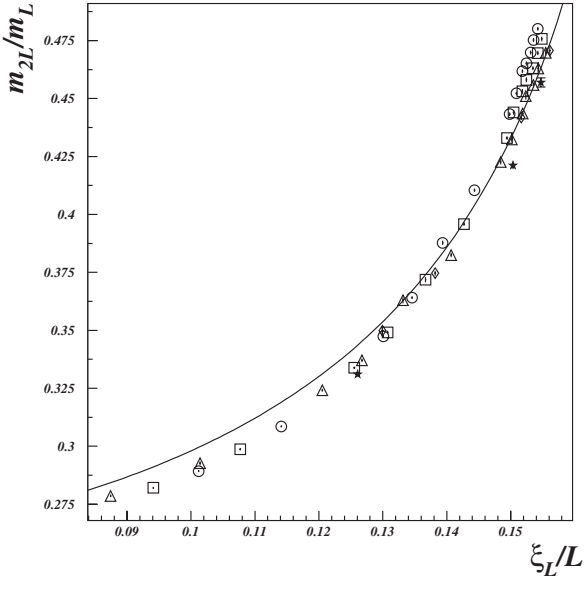

Fig. 6. FSS plot for the magnetization m. Symbols are defined as in Fig. 3. The solid line is the theoretical prediction, cf. Eq. (54).

$\log L_\perp$. If we perform a polynomial fit of the data, we obtain $F_m(2, z^*, S_2) = 0.491(15)$ for $z^* = 1/(2\pi)$. Using Eq. (27) we obtain

$$\frac{\beta_\perp}{\nu_\perp} = 1.023(43). \tag{63}$$

Such a result is in very good agreement with the JSLC prediction $\beta_\perp/\nu_\perp = 1$.

The results for the Binder parameter reported in Fig. 7 show a good scaling behavior, falling onto a single curve with small corrections. By using Eq. (27) we obtain approximately $g(\beta_c; L_\parallel, L_\perp) \sim L_\perp^{-0.45(15)}$. Thus, $g = 0$ at the critical point, in agreement with the JSLC theory that predicts Gaussian transverse fluctuations at the critical point. The value of the exponent is difficult to interpret and we suspect that the Binder parameter is going to zero as some negative power of $\log L_\perp$, which however cannot be distinguished numerically from a small exponent.

Finally, we report results for the parallel correlation length. Figure 8 reports a plot of $\xi_\parallel(\beta; L_\parallel, L_\perp)/L_\parallel$ vs. $\xi_\perp(\beta; L_\parallel, L_\perp)/L_\perp$. There are very large corrections to FSS but the data apparently collapse on a well-defined curve as the size of the lattice increases. This is again a very important test

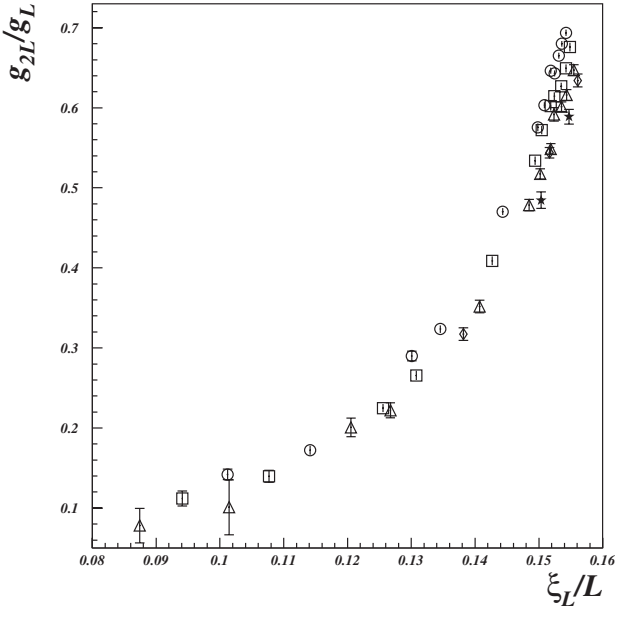

Fig. 7. FSS plot for transverse Binder parameter g. Symbols are defined as in Fig. 3.

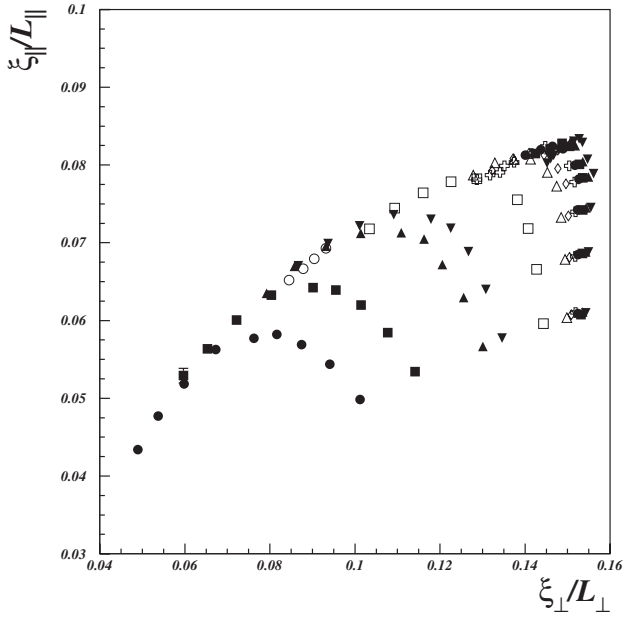

Fig. 8. Plot of $\xi_\parallel(\beta; L_\parallel, L_\perp)/L_\parallel$ versus $\xi_\perp(\beta; L_\parallel, L_\perp)/L_\perp$. Each symbol corresponds to a value of β: 0.28 (●), 0.29 (■), 0.30 (▲), 0.3025 (▼), 0.305 (○), 0.3075 (□), 0.31 (△), 0.3105 (◇), 0.311 (empty cross), 0.31125 (●), 0.3115 (■), 0.31175 (▲), 0.312 (▼). For each β points move leftwards as $L_\parallel$ and $L_\perp$ increase.

of the JSLC theory. Indeed, as discussed in Section 3 the data for the correlation length can both scale only if we have correctly chosen the anisotropy exponent Δ. Thus, Fig. 8, obtained using data with $\Delta = 2$, strongly supports such a value for the anisotropy exponent.

In the JSLC theory the order parameter has the Gaussian distribution (52). However, such an expression does not take into account the presence of the leading corrections and therefore the FSS behavior of the Binder parameter. If we include these terms we expect a more complex form

$$N \exp[-V(|\psi|^2)]\, d\psi\, d\psi^*. \tag{64}$$

For small $|\psi|^2$ it is sensible to expand $V(|\psi|^2)$ in powers of $|\psi|^2$ and thus, if only the lowest moments of $|\psi|^2$ are of interest, we can try to approximate $V(|\psi|^2)$ with its first two terms,

$$V(|\psi|^2) \approx a_2\, |\psi|^2 + a_4\, |\psi|^4, \tag{65}$$

where $a_4/a_2^2 \approx u L_\perp^{-2\sigma}$ times a function of $tL_\perp^2$.

We now show numerically that this approximation describes remarkably well our results for m, $\chi_\perp$, and g: Essentially all corrections to scaling we observe can be taken into account by simply assuming the distribution function (64) and (65).

If we define

$$M_n(z) = \frac{\int d\psi\, d\psi^*\, |\psi|^n\, e^{-|\psi|^2 - z|\psi|^4}}{\int d\psi\, d\psi^*\, e^{-|\psi|^2 - z|\psi|^4}}, \tag{66}$$

then the approximation (65) predicts

$$\begin{aligned} g &= 2 - \frac{M_4(z)}{M_2(z)^2} \\ X &\equiv L_\perp^{d-1} L_\parallel \frac{m^2}{\chi_\perp} = \frac{M_1(z)^2}{M_2(z)}, \end{aligned} \tag{67}$$

where $z = a_4/a_2^2$. Thus, X turns out to be a function of the Binder parameter g, implicitly defined by Eq. (67). In Fig. 9 we report X versus g together with the theoretical prediction (67). The agreement is remarkable, indicating that all corrections are taken into account by a simple generalization of the distribution of the order parameter. Note that, as $g \to 0$, X approaches $\pi/4 \approx 0.785$, which is the value expected for a purely Gaussian distribution.

Finally, we compute β_c from the critical behavior of $\xi_{\perp,\infty}(\beta)$. In order to compute the infinite-volume correlation length, we can use two strategies. One consists in extrapolating $\tau(\beta; L_\parallel, L_\perp)$ to $L_\perp \to \infty$ at fixed S_2. To minimize corrections to scaling we only use the data with $S_2 \approx 0.200$. In Table III we show the results of the fits $\tau(\beta; L_\parallel, L_\perp) = \tau_\infty(\beta) + a(\beta)\, L_\perp^{-2}$ for each β. In all cases we performed several fits, including each time only the results with $L \geqslant L_{\min}$ for increasing $L_{\min}$. The results we report correspond to the fit for which the χ^2 is reasonable, i.e., it is less than the value corresponding to a 95% confidence level. In two cases we have not been able to fulfil this criterion, with a χ^2 which is however only slightly larger. The value of $\tau_\infty(\beta)$ gives the estimate of the infinite-volume correlation length $\xi_{\perp,\infty}(\beta) = 1/\sqrt{\tau_\infty(\beta)}$.

In the previous analysis we have not made any assumption. More precise estimates of $\xi_{\perp,\infty}(\beta)$ can be obtained if we assume the validity of the JSLC theory and use the method of ref. 40 to determine infinite-volume quantities.[12] Such a method is particularly efficient and it has been successfully applied to many different equilibrium models.[43–49] For the calculation we assume here the theoretical prediction for the function $F_\xi(\alpha, z, S_\Delta)$,

[12] A similar method has been introduced in refs. 41 and 42.

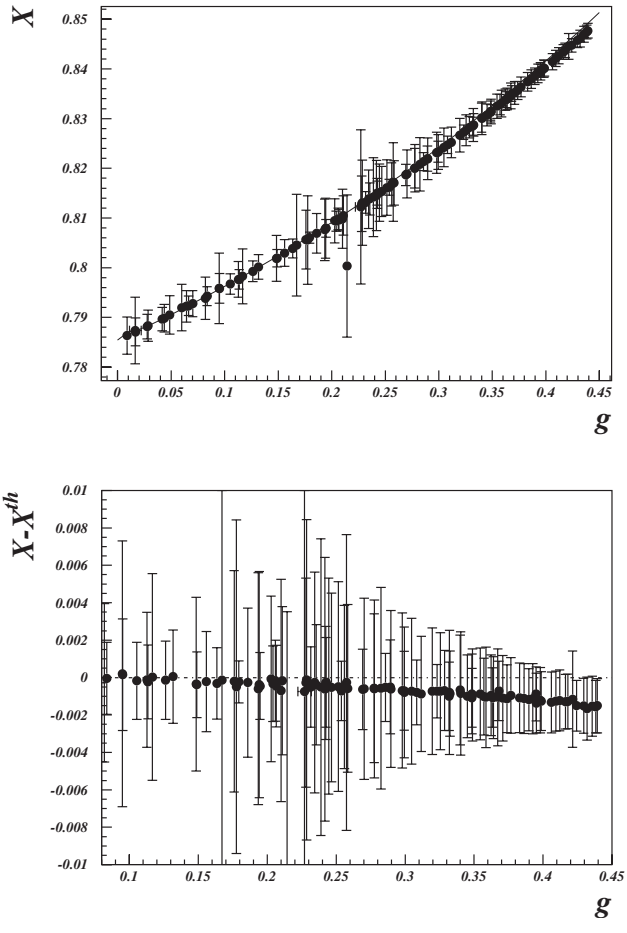

Fig. 9. Upper figure: plot of X vs. g together with the theoretical prediction X th, cf. Eq. (67). Lower figure: plot of $X - X$ th vs. g.

cf. Eq (43), and use the iterative algorithm with $\alpha = 2$. To avoid scaling corrections we only consider the data with $L_\perp \geqslant L_{\min} = 30$ and $S_2 \approx 0.200$. Then, for each β and $L_\perp$ we obtain estimates of $\xi_{\perp,\infty}(\beta)$. Results corresponding to the same β are then combined to give the final estimate reported in Table IV. Here N is the number of degrees of freedom (the number of data with the same β minus one) and R^2 is the sum of square residuals which gives an indication of the consistency of the various extrapolations. The results are in agreement with those previously obtained, but are significantly more precise.

Table III. Fit of $\tau(\beta; L_{\parallel}, L_{\perp})$ with $\tau_{\infty}(\beta) + a(\beta)\, L_{\perp}^{-2}$ Using the Data with $S_2 \approx 0.200$: $L_{\min}$ Is the Minimum Value of L Used in the Fit, N Is the Number of Degrees of Freedom, R^2 Is the χ^2, i.e., the Sum of the Square Residuals, and R_c^2 Is the Value of R^2 Corresponding to the 95% Confidence Level Based on a χ^2 Distribution with N Degrees of Freedom. In the Last Column we Report $\xi^2_{\perp,\infty}(\beta) = 1/\tau_{\infty}(\beta)$

β	$L_{\min}$	N	R^2	R_c^2	τ_{∞}	a	$\xi_{\perp,\infty}(\beta)$
0.28	22	4	3.12	9.49	0.2397(13)	−5.44(87)	2.043(23)
0.29	22	4	2.76	9.49	0.15309(87)	−4.19(56)	2.556(29)
0.3	22	4	5.09	9.49	0.07607(35)	−2.02(24)	3.626(34)
0.3025	22	4	5.19	9.49	0.05864(36)	−1.30(25)	4.130(51)
0.305	24	8	14.63	15.50	0.04382(26)	−1.91(26)	4.777(57)
0.3075	26	2	0.70	6.00	0.02961(52)	−3.33(67)	5.81(20)
0.31	22	4	8.29	9.49	0.01309(11)	0.310(74)	8.74(15)
0.3105	22	4	7.57	9.49	0.01069(18)	0.09(13)	9.67(33)
0.311	24	7	14.78	14.08	0.00852(21)	−0.17(18)	10.83(54)
0.31125	22	4	2.65	9.49	0.00703(11)	−0.012(72)	11.92(39)
0.3115	22	4	8.56	9.49	0.00586(14)	0.01(13)	13.06(63)
0.31175	24	3	9.21	7.82	0.00421(20)	0.49(19)	15.4(1.5)
0.312	28	6	11.46	12.59	0.00348(16)	0.01(20)	17.0(1.5)

Table IV. Results of the Extrapolation with the Iterative Method of Ref. 40 Using the Theoretical FSS Function. Here N Is the Number of Points for Each β, R^2 the Residual, and R_c^2 Is the Value Corresponding to a 95% Confidence Level

β	$\xi_{\perp,\infty}(\beta)$	N	R^2	R_c^2
0.28	2.0603(39)	3	1.1	7.8
0.29	2.5850(50)	3	1.5	7.8
0.3	3.6702(52)	3	3.8	7.8
0.3025	4.1668(88)	3	5.6	7.8
0.305	4.8474(92)	8	18.1	15.5
0.3075	6.040(20)	3	6.4	7.8
0.31	8.673(34)	3	2.8	7.8
0.3105	9.654(54)	3	3.8	7.8
0.311	10.866(45)	7	19.9	14.1
0.31125	11.97(11)	3	0.6	7.8
0.3115	13.07(10)	3	5.4	7.8
0.31175	14.81(16)	3	2.8	7.8
0.312	17.00(16)	7	5.3	14.1

Once $\xi_{\perp,\infty}(\beta)$ has been computed, we have first performed fits of the form

$$\xi_{\perp,\infty}(\beta) = \tilde{A}\left(1-\frac{\beta}{\beta_c}\right)^{-\nu_\perp}, \tag{68}$$

using only the data with $\beta \geqslant \beta_{\min}$. The value $\beta_{\min}$ corresponds to the lowest value for which the χ^2 is less than the value corresponding to a 95% confidence level. Using the first set of extrapolated values, see Table III, we obtain $\nu_\perp = 0.483(50)$, $\beta_c = 0.31264(15)$, while the second set, see Table IV, gives $\nu_\perp = 0.500(32)$ and $\beta_c = 0.312696(88)$. The results are in full agreement with the prediction $\nu_\perp = 1/2$. Of course, in the second case this is simply a consistency check, since, by using the theoretical prediction for the scaling curve, we have implicitly assumed $\nu_\perp = 1/2$.

In order to obtain our best estimate of β_c, we fix $\nu_\perp = 1/2$ and use the second set of extrapolations (which have been performed implicitly assuming $\nu_\perp = 1/2$). Still fitting with Eq. (68), we obtain for $\beta_{\min} = 0.31$

$$\beta_c = 0.312694(18), \tag{69}$$

with $\chi^2 = 6.0$ and 5 degrees of freedom. The addition of an analytic correction does not improve substantially the result.

The result for β_c should be compared with the existing determinations:

$$\beta_c = \begin{cases} 0.3108(11) & \text{(ref. 50);} \\ 0.3125(13) & \text{(ref. 15);} \\ 0.3156(9) & \text{(ref. 20);} \\ 0.3125(10) & \text{(ref. 21).} \end{cases} \tag{70}$$

Our result (69) and the estimates of refs. 15, 21, and 50 are in reasonable agreement. On the other hand, the estimate of ref. 20 is sligthly larger, although the difference (three error bars) is not yet very significant.

6. CONCLUSIONS

In this paper we have performed a thorough check of the theoretical predictions for the DLG. We have verified that the FSS curves $F(2, z, S_\Delta)$ for $\chi_\perp$ and $\xi_\perp$ agree with the JSLC predictions (43) and (44) if Δ is fixed to the JSLC value $\Delta = 2$. We wish to stress that the comparison between theory and numerical data does not require any tuning of parameters, at variance with previous studies in which the FSS analysis required fixing β_c and/or some exponents. We also analyzed the magnetization at the critical

point finding $\beta_\perp/\nu_\perp = 1.023(43)$, in agreement with the JSLC value $\beta_\perp/\nu_\perp = 1$. Our results for the Binder parameter g do not agree with those of ref. 14 where it was found $g \neq 0$ at criticality, but confirm the results of Wang[15] who could not find a satisfactory collapse for the Binder parameter. Our result $g = 0$ is compatible with the idea that even finite-volume transverse correlations are Gaussian in the scaling limit, so that $g = 0$ at criticality. Finally, we discuss the FSS behavior of the magnetization. Our results are consistent with a Gaussian distribution for the order parameter with corrections that are well parametrized in terms of the Binder parameter.

One point that is still unclear is the role of the dangerously irrelevant operator. A general analysis confirmed by an explicit one-loop computation indicates that this operator does not give rise to FSS violations in any $2 < d < 5$. However, in two dimensions the same arguments predict logarithmic violations (if it is marginally relevant) or at least logarithmic corrections (if it is marginally irrelevant). Numerically, we observe corrections to the Gaussian field-theoretical predictions but we are not able to determine their behavior as $L_\perp \to \infty$. Indeed, very large lattices are needed to distinguish logarithmic corrections from power-law corrections with small exponents. In any case, our data indicate that the operator is marginally irrelevant since $g \to 0$ as $L_\perp \to 0$. We find $\gamma_g/\nu_\perp = 0.45(15)$ but this result should not be taken seriously. Probably, g decreases as a power of $\log L$ because of the marginal operator, but, in our range of values of $L_\perp$, the complicated logarithmic dependence is mimicked by a single power. Note that, if $g(\beta_c; \infty, \infty) = 0$, the Binder parameter cannot be used to compute β_c: the crossing method does not work.

Let us now compare our results with those of refs. 20 and 21 that presented numerical results apparently in good agreement with the RDLG scenario. If the JSLC theory gives the correct description of the critical behavior, the family of lattices considered in ref. 20—at fixed $\Delta = 1$—is such that $L_\perp$ increases too fast compared to $L_\parallel$. As discussed in ref. 31, in this case one expects to observe scaling with an effective geometry corresponding to $L_\perp = \infty$. Therefore, longitudinal quantities should show the correct behavior, i.e., with the JSLC exponents, when studied in terms of $(\beta - \beta_c)\, L_\parallel^{1/\nu_\parallel}$. On the other hand, transverse quantities should have a critical behavior with effective exponents. Therefore, there is no contradiction with the estimates of ref. 20 that differ from the JSLC ones. It is also useful to take the opposite point of view: What should our results be if the DLG belongs to the same universality class as the RDLG? If this were the case, the correct anisotropy exponent would be $\Delta = 1$. Thus, the lattices we consider are such that $L_\parallel$ increases too fast compared to $L_\perp$. Again, we expect to observe scaling,[31] with an effective geometry $L_\parallel = \infty$. Transverse quantities should have the correct behavior, i.e., transverse critical exponents

should coincide with those of the theory with $\Delta = 1$. Therefore, our results should be the same as those of ref. 20, which, as we have shown here, is not the case. Thus, our data exclude $\Delta = 1$. As discussed in ref. 31, it is possible to determine Δ unambiguously from the FSS behavior of $\xi_{\parallel}$ and of $\xi_{\perp}$. Indeed, only if Δ is chosen correctly, both correlations length scale linearly, i.e., $\xi_{\perp} \sim L_{\perp}$ and $\xi_{\parallel} \sim L_{\parallel}$. This is indeed what we have checked in Section 5.2. Therefore, our data strongly support the JSLC prediction $\Delta = 2$, and do not support the claim of ref. 20 that the DLG and the RDLG belong to the same universality class.

Finally, let us discuss[51] the results of Albano and Saracco.[21] First of all, there is a serious flaw in one of their scaling Ansätze, due to the fact that they do not distinguish between $z_{\perp}$ and $z_{\parallel}$.[3] While in their Eqs. (5), (6), and (7) the exponent z should be identified with $z_{\parallel}$ (the JSLC prediction is $z_{\parallel} = 4/3$ as correctly appears in their Table I), in Eqs. (8), (9), and (10), the exponent z should be identified with $z_{\perp}$ (the JSLC prediction is $z_{\perp} = 4$). Therefore, their result for $c_{\perp}$ does not agree with any prediction, neither the JSLC one nor the RDLG one. Moreover, with the lattice sizes they consider, it is not clear whether they are really looking at the short-time dynamics in infinite volume or rather to the approach to equilibrium in a finite lattice. Indeed, since the dynamics in the longitudinal direction is fast, one expects to generate correlations of size $L_{\parallel}$ in a time of order $L_{\parallel}^{z_{\parallel}}$, so that a necessary condition to avoid size effect is that $t \ll L_{\parallel}^{z_{\parallel}}$. With their typical lattice sizes, one would expect to avoid size effects for $t \lesssim 10^2$. If larger values of t are used—they consider times up to 10^4—finite-size effects are relevant and thus, contrary to their claims, the aspect ratio and the value of the anisotropy exponent become again a crucial issue.

APPENDIX A. BINDER CUMULANT WITHOUT ZERO MODE

In Section 4 we stated that the Gaussian nature of the transverse fluctuations implies that the Binder cumulant vanishes at criticality. We consider now the $O(N)$ model for $N \to \infty$ above the upper critical dimension ($d > 4$), showing that the Binder cumulant defined in Eq. (13) also vanishes, in spite of the presence of the dangerously irrelevant operator. This is due to the fact that the definition (13) involves the correlation functions at nonvanishing momenta.

To be concrete let us consider the $O(N)$ σ-model defined on a finite hypercubic lattice Λ of volume L^d, with Hamiltonian

$$\mathscr{H} = -N \sum_{\langle \mathbf{x}, \mathbf{y} \rangle} \boldsymbol{\sigma}_{\mathbf{x}} \cdot \boldsymbol{\sigma}_{\mathbf{y}}, \tag{71}$$

where $\langle \cdot, \cdot \rangle$ indicates nearest-neighbor sites. The partition function is simply

$$Z = \int \prod_{\mathbf{x}} [\mathrm{d}\boldsymbol{\sigma}_{\mathbf{x}}\, \delta(\boldsymbol{\sigma}_{\mathbf{x}}^2 - 1)]\, e^{-\beta \mathscr{H}} \times \begin{cases} 1 & \text{ZM} \\ \delta(\sum_{\mathbf{x}} \boldsymbol{\sigma}_{\mathbf{x}}) & \text{ZM} \end{cases} \tag{72}$$

where $\beta \equiv 1/T$, ZM corresponds to the standard case (with zero mode), and ZM to the theory without zero mode. The Fourier transform of the two-point correlation function is given by

$$G^{\alpha,\beta}(\mathbf{p}) \equiv \langle \sigma^{\alpha}_{-\mathbf{p}} \sigma^{\beta}_{\mathbf{p}} \rangle_{\Lambda} = \frac{1}{\beta} \frac{\delta_{\alpha,\beta}}{\hat{\mathbf{p}}^2 + \lambda_L} \times \begin{cases} 1 & \text{ZM} \\ 1 - \delta_{\mathbf{p},\mathbf{0}} & \text{ZM} \end{cases} \tag{73}$$

where $\hat{\mathbf{p}}^2 = 4 \sum_{\mu} \sin^2(p_{\mu}/2)$ and $\lambda_L = \lambda_L(\beta, L)$ solves the finite-volume gap equation of the model

$$\beta = \frac{1}{L^d} \sum_{\mathbf{p} \in \Lambda^*} \frac{1}{\hat{\mathbf{p}}^2 + \lambda_L} \times \begin{cases} 1 & \text{ZM} \\ 1 - \delta_{\mathbf{p},\mathbf{0}} & \text{ZM} \end{cases} \tag{74}$$

in which $\Lambda^* = 2\pi L^{-1}\, \mathbb{Z}_L^d$ is the dual lattice.

We now define two different Binder cumulants

$$\begin{aligned} g_0(\beta, L) &= -\frac{1}{L^d} \frac{\langle (\mathbf{m} \cdot \mathbf{m})^2 \rangle_c}{\langle \mathbf{m} \cdot \mathbf{m} \rangle_c^2}, \\ g_1(\beta, L) &= -\frac{1}{L^d} \frac{\langle (\boldsymbol{\mu} \cdot \boldsymbol{\mu})^2 \rangle_c}{\langle \boldsymbol{\mu} \cdot \boldsymbol{\mu} \rangle_c^2}, \end{aligned} \tag{75}$$

where $m^{\alpha} \equiv \sigma^{\alpha}_{\mathbf{p}=\mathbf{0}}$, $\mu^{\alpha} \equiv \sigma^{\alpha}_{\mathbf{p}=\mathbf{p}_{\min}}$, and $|\mathbf{p}_{\min}| = 2\pi/L$. The definition $g_0(\beta, L)$ is the one usually used in the N-vector model, but it is unsuitable for systems without zero mode. In this case, the natural definition is $g_1(\beta, L)$ and indeed such a quantity corresponds to the Binder cumulant we have used in the DLG simulation, cf. Eq. (13).

Now, let us compute $g_{0,1}(\beta_c, L)$ for $d > 4$ at the critical point β_c,

$$\beta_c = \int_{-\pi}^{\pi} \frac{\mathrm{d}^d q}{(2\pi)^d} \frac{1}{\hat{\mathbf{q}}^2}. \tag{76}$$

In ref. 26 we found that, for $d > 4$,

$$\lambda_L(\beta_c, L) = \begin{cases} \mathscr{C}_{d,1}^{-1/2} L^{-d/2} [1 + O(L^{2-d/2})] & \text{ZM} \\ \mathscr{I}(0)/\mathscr{C}_{d,1} L^{2-d} [1 + O(L^{4-d})] & \text{ZM} \end{cases} \tag{77}$$

where $\mathscr{C}_{d,1}$ and $\mathscr{I}(\rho)$ are defined in Eqs. (2.19) and (A.5) of ref. 26, respectively. This is sufficient to determine the behavior of $\langle \mathbf{m}\cdot\mathbf{m}\rangle_c$ and $\langle \boldsymbol{\mu}\cdot\boldsymbol{\mu}\rangle_c$ at (bulk) criticality. As far as the four-point function is concerned, it can be expressed in terms of

$$\Delta^{-1}(\mathbf{q}) \equiv \frac{1}{2\beta^2}\frac{1}{L^d}\sum_{\mathbf{p}\in\Delta^*}\frac{1}{[\hat{\mathbf{p}}+\mathbf{q}^2+\lambda_L][\hat{\mathbf{p}}^2+\lambda_L]}\times\begin{cases}1 & \text{ZM}\\ (1-\delta_{\mathbf{p},0})(1-\delta_{\mathbf{p}+\mathbf{q},0}) & \text{Z}\not{\text{M}}.\end{cases} \tag{78}$$

After some calculation one can easily show that, at criticality and with $|\mathbf{q}|\sim 1/L$,

$$\Delta^{-1}(\mathbf{q})|_{\beta_c} = \frac{\mathscr{C}_{d,1}}{2\beta_c^2}(1+\delta_{\mathbf{q},0}) + \begin{cases}O(L^{2-d/2}) & \text{ZM}\\ O(L^{4-d}) & \text{Z}\not{\text{M}}.\end{cases} \tag{79}$$

In the large N-limit we have

$$\langle \boldsymbol{\sigma}_{-\mathbf{q}}\cdot\boldsymbol{\sigma}_{\mathbf{q}}\rangle_c = NG^{1,1}(\mathbf{q}) + O(N^0), \tag{80}$$

$$\langle (\boldsymbol{\sigma}_{-\mathbf{q}}\cdot\boldsymbol{\sigma}_{\mathbf{q}})^2\rangle_c = -(N+2)\,\Delta(\mathbf{q})[G^{1,1}(\mathbf{q})]^4 + O(N^0), \tag{81}$$

so that

$$g_0(\beta_c, L) = \frac{N+2}{N^2}[1+O(L^{2-d/2}, N^{-2})], \qquad \text{ZM} \tag{82}$$

$$g_1(\beta_c, L) = O(N^{-1}L^{4-d}). \qquad \text{ZM, Z}\not{\text{M}}. \tag{83}$$

The different scaling behavior can be traced back to the fact that, while the four-point function has always the same scaling behavior, irrespective of the momentum at which it is computed, the two-point function scales differently (for $d>4$) depending on whether it is computed at zero or at nonzero momentum.

It is also of interest to compute the Binder parameter in $d=4$. Without reporting the details, we find that $g_0(\beta_c, L)$ agrees with the result reported above, with logarithmic corrections. For $g_1(\beta_c, L)$ we obtain instead

$$g_1(\beta, L) \approx \frac{N+2}{N^2}\frac{1}{\pi^2 \log L}. \tag{84}$$

The Binder cumulant $g_1(\beta, L)$ vanishes also in $d=4$, albeit only logarithmically.

APPENDIX B. DANGEROUSLY IRRELEVANT OPERATOR AND CORRELATION FUNCTIONS

In this Appendix we compute the zero-momentum insertion of the dangerously irrelevant operator $\mathscr{A}$ into static correlation functions of n density fields s taken at vanishing parallel momenta in the JSLC theory.[6][13] We begin by considering $\varphi(\mathbf{p}, \omega) \equiv s(p_{\parallel} = 0, \mathbf{p}_{\perp} = \mathbf{p}, \omega)$, i.e., we compute

$$\langle \varphi(\mathbf{p}_1, \omega_1) \cdots \varphi(\mathbf{p}_n, \omega_n)\, \mathscr{A} \rangle_{\text{conn}}. \tag{85}$$

We recall that the interaction vertex $\mathscr{V}$ of the theory[6] is $\tilde{s}\, \nabla_{\parallel} s^2$ ($\tilde{s}$ is the response field) and thus it vanishes whenever the parallel momenta flowing into it from the $\tilde{s}$-leg is zero. Let us discuss the consequences of this fact on the form of the generic diagram $\mathscr{D}$ contributing to Eq. (85).

First, note that if the amputated diagram $\mathscr{D}^{\text{amp}}$ associated with $\mathscr{D}$ has no external $\tilde{s}$-legs, it contains a loop of response propagators and therefore it vanishes because of causality.[33–35] Thus $\mathscr{D}$ vanishes unless $\mathscr{D}^{\text{amp}}$ has at least one external $\tilde{s}$-leg. Each external $\tilde{s}$-leg in $\mathscr{D}^{\text{amp}}$ is connected either to the insertion $\mathscr{A}$ or to an interaction vertex $\mathscr{V}$. In the latter case, however, the contribution vanishes because of the zero parallel momentum flowing from the external $\tilde{s}$-leg into the vertex $\mathscr{V}$. Thus, $\mathscr{D}$ does not vanish only if each of the $\tilde{n} \geqslant 1$ external $\tilde{s}$-legs of $\mathscr{D}^{\text{amp}}$ belongs to the insertion of $\mathscr{A}$. Now we show that $\mathscr{D}^{\text{amp}}$ cannot be one-particle reducible. Indeed, let us suppose that $\mathscr{D}^{\text{amp}}$ can be divided into two amputated subdiagrams $\mathscr{D}_1^{\text{amp}}$ and $\mathscr{D}_2^{\text{amp}}$, such that $\mathscr{A} \in \mathscr{D}_1^{\text{amp}}$, connected with a single line. By momentum conservation, the parallel momentum flowing into this line is zero and therefore such a line must be connected to an s-leg of a vertex in $\mathscr{D}_2^{\text{amp}}$. Since we also have $\mathscr{A} \in \mathscr{D}_1^{\text{amp}}$, all external legs of $\mathscr{D}_2^{\text{amp}}$ are of s-type. By causality $\mathscr{D}_2^{\text{amp}}$ vanishes.

Summing up, the amputated diagrams contributing to Eq. (85) are one-particle irreducible and all the $\tilde{n} \geqslant 1$ external $\tilde{s}$-legs belong to the insertion of $\mathscr{A}$.

This conclusion is independent of the particular $\mathscr{A}$ considered. Now let us specify our discussion to the case of the dangerously irrelevant operator. The dangerous irrelevant coupling $\tilde{s}\, \Delta_{\perp} s^3$ mixes, under renormalization-group transformations, with other operators of equal or smaller scaling dimension. Those with the same dimension, that we consider in the following, are listed in ref. 6. They have the following general structure (the dots indicate derivatives): (a) $\tilde{s}(\cdots)\, s$, (b) $\tilde{s}(\cdots)\, \tilde{s}$, (c) $\tilde{s}\, \nabla_{\parallel}(\cdots)\, s^2$, (d) $\tilde{s}(\cdots)\, s^3$. For $n > 2$, the only case we consider, the insertion of one of the operators (a) or (b) into the correlation function gives only one-particle

[13] In this Appendix we use the notations of ref. 6.

reducible contributions since one of their $\tilde{s}$-legs has to be an external one for the amputated diagram.[14] Thus, according to our previous discussion, they do not contribute to the correlation function. The same is true for operators (c). The $\tilde{s}$-leg, being an external one for the amputated diagram, carries a zero parallel momentum $p_\parallel$ into the vertex. Since these vertices are proportional to $p_\parallel$, they vanish. Thus, contributions can only come from $\tilde{s}\,\Delta_\perp s^3 \in \mathscr{A}$. Defining

$$B_3 \equiv \tfrac{1}{6}\int \mathrm{d}t\, \mathrm{d}^d x\, \tilde{s}\,\Delta_\perp s^3, \tag{86}$$

we obtain

$$\langle \varphi(\mathbf{p}_1, \omega_1)\cdots\varphi(\mathbf{p}_n, \omega_n)\,\mathscr{A}\rangle_{\text{conn, amp}} = u\Gamma_{1,n-1;B_3}, \tag{87}$$

where $\Gamma_{\tilde{n},n;B_3}$ is the one-particle irreducible vertex function with $\tilde{n}$ external $\tilde{s}$-legs, n external s-legs, and one (zero-momentum) insertion of the operator B_3, $\mathscr{A} \approx uB_3 + \cdots$. Therefore, all connected correlation functions with vanishing parallel momenta and $n > 2$ are proportional to u as $u \to 0$.

We wish now to compute the transverse static four-point function $\tilde{G}^{(4)}(\mathbf{p}, \mathbf{p}, -\mathbf{p}, -\mathbf{p}; L_\parallel, L_\perp)$ at zero parallel momenta. For simplicity, we restrict the computation to $\tau = 0$, i.e., to the critical point. The tree-level insertion of B_3 into the four-point correlation functions with all fields s taken at the same value of t (we can set $t = 0$) and with momenta $\mathbf{P} = (0, \mathbf{p}_\perp)$ is given by

$$\mathscr{D}_{\text{TL}} = 4u\mathbf{p}_\perp^2 \int_{-\infty}^{+\infty} \mathrm{d}t_i\, R(-t_i, \mathbf{P})\, C^3(-t_i, \mathbf{P}) = \frac{u}{(\mathbf{p}_\perp^2)^4}, \tag{88}$$

where we have used[15] (see ref. 6)

$$\begin{aligned} R(t_1 - t_2, \mathbf{q}) &= \langle \tilde{s}(t_2, -\mathbf{q})\, s(t_1, \mathbf{q})\rangle_{\text{TL}} \\ &= \theta(t_1 - t_2)\exp\{-[\mathbf{q}_\perp^4 + q_\parallel^2](t_1 - t_2)\} \end{aligned} \tag{89}$$

$$\begin{aligned} C(t_1 - t_2, \mathbf{q}) &= \langle s(t_2, -\mathbf{q})\, s(t_1, \mathbf{q})\rangle_{\text{TL}} \\ &= \frac{\mathbf{q}_\perp^2}{\mathbf{q}_\perp^4 + q_\parallel^2}\exp\{-[\mathbf{q}_\perp^4 + q_\parallel^2]\,|t_1 - t_2|\}, \end{aligned} \tag{90}$$

and $\theta(t)$ is the Heaviside step function.

[14] For $n = 2$ (a) and (b) have nonzero tree-level contributions.
[15] We disregard dimensionless factors present in the dynamic functional of ref. 6.

At one loop there are two diagrams whose contributions can be written in the form

$$L_1(t_1, t_2, t_3; \mathbf{p}_\perp)$$

$$= -g^2 \frac{1}{V} \sum_{(q_\parallel, \mathbf{q}_\perp)}{}' \mathbf{q}_\parallel^{1,2} \mathbf{q}_\parallel^{1,3} R(t_1 - t_2, \mathbf{q}^{1,2})\, R(t_1 - t_3, \mathbf{q}^{1,3})\, C(t_2 - t_3, \mathbf{q}^{2,3}), \quad (91)$$

$$L_2(t_1, t_2, t_3; \mathbf{p}_\perp)$$

$$= -g^2 \frac{1}{V} \sum_{(q_\parallel, \mathbf{q}_\perp)}{}' \mathbf{q}_\parallel^{1,2} \mathbf{q}_\parallel^{2,3} R(t_1 - t_2, \mathbf{q}^{1,2})\, R(t_2 - t_3, \mathbf{q}^{2,3})\, C(t_1 - t_3, \mathbf{q}^{1,3}), \quad (92)$$

where $\sum'$ runs over the whole momentum space *except* the zero mode $(0, \mathbf{0})$ *and* $(0, \pm \mathbf{p}_\perp)$, and

$$\mathbf{q}^{1,2} = (q_\parallel, \mathbf{q}_\perp + \mathbf{p}_\perp), \quad (93)$$

$$\mathbf{q}^{1,3} = (-q_\parallel, -\mathbf{q}_\perp + \mathbf{p}_\perp), \quad (94)$$

$$\mathbf{q}^{2,3} = (q_\parallel, \mathbf{q}_\perp). \quad (95)$$

The final result is given by $T = T_1 + T_2$ where we defined

$$T_i(\mathbf{p}_\perp) = \gamma_i u \mathbf{p}_\perp^2 \int_{-\infty}^{+\infty} \mathrm{d}t_1\, \mathrm{d}t_2\, \mathrm{d}t_3\, L_i(t_1, t_2, t_3; \mathbf{p}_\perp)\, R(-t_1, \mathbf{P}) \prod_{k=1}^{3} C(-t_k, \mathbf{P}), \quad (96)$$

and $\gamma_1 = 4!/2$, $\gamma_2 = 2\gamma_1$ are combinatorial factors. Performing the integrations over t_i, it is easy to find

$$T(\mathbf{p}_\perp) = \frac{\gamma_1}{2} g^2 \frac{u}{(\mathbf{p}_\perp^2)^3} \frac{1}{V} \sum_{(q_\parallel, \mathbf{q}_\perp)}{}' f(\mathbf{q}, \mathbf{p}_\perp), \quad (97)$$

with $f(\mathbf{q}, \mathbf{p}_\perp = \mathbf{0}) \neq 0$ and $f((\lambda^2 q_\parallel, \lambda \mathbf{q}_\perp), \mathbf{p}_\perp) \sim \lambda^{-8}$ for large λ. The sum over $f(\mathbf{q}, \mathbf{p}_\perp)$ is convergent by power counting (for $d < 7$) and thus, for $|p_\perp| \to 0$,

$$\sum_{(q_\parallel, \mathbf{q}_\perp)}{}' f(\mathbf{q}, \mathbf{p}_\perp) \approx \sum_{(q_\parallel, \mathbf{q}_\perp)}{}' f(\mathbf{q}, 0) \sim L_\perp^8. \quad (98)$$

Then, if $|\mathbf{p}_\perp| \sim 1/L_\perp$, it is easy to see that, for $d = 5$ and at $S = L_\perp^2 / L_\parallel$ fixed (thus $V = L_\perp^{d+1}/S$), T is finite and

$$T \sim \mathscr{D}_{\mathrm{TL}} \sim L_\perp^8 \quad (99)$$

in agreement with Eq. (50).

ACKNOWLEDGMENTS

It is a pleasure to thank Beate Schmittmann and Royce Zia for many useful discussions and Miguel Muñoz for correspondence. We acknowledge the support of the Istituto Nazionale Fisica della Materia (INFM) through the Advanced Parallel Computing Project at CINECA. These computations were carried out in part on the Computational Physics Cluster at New York University, which was supported by NSF Grant PHY–0116590.

REFERENCES

1. B. Derrida, J. L. Lebowitz, and E. R. Speer, *Phys. Rev. Lett.* **87**:150601 (2001); *J. Stat. Phys.* **107**:599 (2002); *Phys. Rev. Lett.* **89**:030601 (2002); *J. Stat. Phys.* **110**:775 (2003); L. Bertini, A. De Sole, D. Gabrielli, G. Jona-Lasinio, and C. Landim, *Phys. Rev. Lett.* **87**:040601 (2001); *J. Stat. Phys.* **107**:635 (2002). For an overview see D. Ruelle, *Nature* **411**:27 (2001).
2. S. Katz, J. L. Lebowitz, and H. Spohn, *Phys. Rev. B* **28**:1655 (1983); *J. Stat. Phys.* **34**:497 (1984).
3. B. Schmittmann and R. K. P. Zia, Statistical mechanics of driven diffusive systems, in *Phase Transitions and Critical Phenomena*, C. Domb and J. L. Lebowitz, eds., Vol. 17 (Academic, London, 1995). R. K. P. Zia, Driven diffusive systems: A tutorial and recent developments, in *Computer Simulations of Surfaces and Interfaces*, D. P. Landau, A. I. Milchev, and B. Dünweg, eds., NATO Science Series II, Vol. 114 (Kluwer, Dordrecht, 2003), available at www.phys.vt.edu/~rkpzia/RCP.html.
4. J. Marro and R. Dickman, *Nonequilibrium Phase Transitions in Lattice Models* (Cambridge University Press, Cambridge, 1999).
5. H. van Beijeren and L. S. Schulman, *Phys. Rev. Lett.* **53**:806 (1984).
6. H. K. Janssen and B. Schmittmann, *Z. Phys. B* **64**:503 (1986).
7. K.-t. Leung and J. L. Cardy, *J. Stat. Phys.* **44**:567 (1986); Erratum, *J. Stat. Phys.* **45**:1087 (1986).
8. P. L. Garrido, F. de los Santos, and M. A. Muñoz, *Phys. Rev. E* **57**:752 (1998).
9. P. L. Garrido and F. de los Santos, *J. Stat. Phys.* **96**:303 (1999), e-print cond-mat/9805211.
10. P. L. Garrido, M. A. Muñoz, and F. de los Santos, *Phys. Rev. E* **61**:R4683 (2000), e-print cond-mat/0001165.
11. B. Schmittmann, H. K. Janssen, U. C. Täuber, R. K. P. Zia, K.-t. Leung, and J. L. Cardy, *Phys. Rev. E* **61**:5977 (2000), e-print cond-mat/9912286.
12. K.-t. Leung, *Phys. Rev. E* **63**:016102 (2001), e-print cond-mat/0006217.
13. M. Q. Zhang, J.-S. Wang, J. L. Lebowitz, and J. L. Vallés, *J. Stat. Phys.* **52**:1461 (1988).
14. K.-t. Leung, *Int. J. Mod. Phys. C* **3**:367 (1992).
15. J. S. Wang, *J. Stat. Phys.* **82**:1409 (1996).
16. K.-t. Leung and J. S. Wang, *Int. J. Mod. Phys. C* **10**:853 (1999), e-print cond-mat/9805285.
17. K. Binder and J. S. Wang, *J. Stat. Phys.* **55**:87 (1989).
18. B. Schmittmann and R. K. P. Zia, *Phys. Rev. Lett.* **66**:357 (1991).
19. B. Schmittmann, *Europhys. Lett.* **24**:109 (1993).
20. A. Achahbar, P. L. Garrido, J. Marro, and M. A. Muñoz, *Phys. Rev. Lett.* **87**:195702 (2001), e-print cond-mat/0106470.

21. E. V. Albano and G. Saracco, *Phys. Rev. Lett.* **88**:145701 (2002), e-print cond-mat/0210141.
22. M. A. Muñoz, *Some Puzzling Problems in Nonequilibrium Field Theories*, e-print cond-mat/0210645.
23. P. L. Garrido, J. L. Lebowitz, C. Maes, and H. Spohn, *Phys. Rev. A* **42**:1954 (1990).
24. G. Grinstein, *J. Appl. Phys.* **69**:5441 (1991).
25. J. L. Vallés and J. Marro, *J. Stat. Phys.* **43**:441 (1986); **49**:89 (1987).
26. S. Caracciolo, A. Gambassi, M. Gubinelli, and A. Pelissetto, *Eur. Phys. J. B* **20**:255 (2001), e-print cond-mat/0010479.
27. S. Caracciolo, A. Gambassi, M. Gubinelli, and A. Pelissetto, *J. Phys. A* **36**, L315 (2003), e-print cond-mat/0211669.
28. K. Kawasaki, in *Phase Transitions and Critical Phenomena*, C. Domb and M. S. Green, eds., Vol. 2 (Academic, New York, 1972), p. 443.
29. M. E. Fisher, in *Critical Phenomena*, International School of Physics Enrico Fermi, Course LI, M. S. Green, ed. (Academic, New York, 1971).
30. M. N. Barber, Finite-size scaling, in *Phase Transitions and Critical Phenomena*, C. Domb and J. L. Lebowitz, eds., Vol. 8 (Academic, London, 1983).
31. S. Caracciolo, A. Gambassi, M. Gubinelli, and A. Pelissetto, *Eur. Phys. J. B* **34**:205 (2003), e-print cond-mat/0304297.
32. K. Gawedzki and A. Kupiainen, *Nucl. Phys. B* **269**:45 (1986).
33. H. K. Janssen, *Z. Phys. B* **23**:377 (1976).
34. R. Bausch, H. K. Janssen, and H. Wagner, *Z. Phys. B* **24**:113 (1976).
35. H. K. Janssen, Field-theoretic method applied to critical dynamics, in *Dynamical Critical Phenomena and Related Topics*, C. P. Enz, ed., Lecture Notes in Physics, Vol. 104 (Springer, Berlin-New York-Tokyo, 1979).
36. J. Zinn-Justin, *Quantum Field Theory and Critical Phenomena*, 4th ed. (Oxford Science Publication, Clarendon Press, Oxford, 2001).
37. E. Brézin, *J. Physique* **43**:15 (1982).
38. B. Efron, *The Jackknife, the Bootstrap, and Other Resampling Plans*, Regional Conference Series in Applied Mathematics, Vol. 38 (SIAM, Philadelphia, 1982).
39. S. Caracciolo and A. Pelissetto, *Phys. Rev. D* **58**:105007 (1998).
40. S. Caracciolo, R. G. Edwards, S. J. Ferreira, A. Pelissetto, and A. D. Sokal, *Phys. Rev. Lett.* **74**:2969 (1995), e-print hep-lat/9409004.
41. M. Lüscher, P. Weisz, and U. Wolff, *Nucl. Phys. B* **359**:221 (1991).
42. J.-K. Kim, *Europhys. Lett.* **28**:211 (1994); *Phys. Rev. D* **50**:4663 (1994); *Nucl. Phys. B (Proc. Suppl.)* **34**:702 (1994).
43. S. Caracciolo, R. G. Edwards, A. Pelissetto, and A. D. Sokal, *Phys. Rev. Lett.* **75**:1891 (1995), e-print hep-lat/9411009.
44. S. Caracciolo, R. G. Edwards, T. Mendes, A. Pelissetto, and A. D. Sokal, *Nucl. Phys. B (Proc. Suppl.)* **47**:763 (1996), e-print hep-lat/9509033.
45. G. Mana, A. Pelissetto, and A. D. Sokal, *Phys. Rev. D* **54**:1252 (1996), e-print hep-lat/9602015.
46. T. Mendes, A. Pelissetto, and A. D. Sokal, *Nucl. Phys. B* **477**:203 (1996), e-print hep-lat/9604015.
47. G. Mana, A. Pelissetto, and A. D. Sokal, *Phys. Rev. D* **55**:3674 (1997), e-print hep-lat/9610021.
48. S. J. Ferreira and A. D. Sokal, *J. Stat. Phys.* **96**:461 (1999), e-print cond-mat/9811345.
49. S. Caracciolo and M. Palassini, *Phys. Rev. Lett.* **82**:5128 (1999), e-print cond-mat/9904246.
50. K.-t. Leung, *Phys. Rev. Lett.* **66**:453 (1991).
51. S. Caracciolo, A. Gambassi, M. Gubinelli, and A. Pelissetto, *Phys. Rev. Lett.* **92**:029601 (2004), e-print cond-mat/0305213.